科技部補助專題研究計畫成果報告
期末報告

香菸煙霧水提取物造成人類血管內皮細胞及斑馬魚幼蟲發炎特性及保健防治研究(第 2 年)

計 畫 類 別 ： 個別型計畫
計 畫 編 號 ： NSC 101-2320-B-040-019-MY2
執 行 期 間 ： 102 年 08 月 01 日至 103 年 07 月 31 日
執 行 單 位 ： 中山醫學大學生物醫學科學學系（所）

計 畫 主 持 人 ： 王祖興

計畫參與人員： 碩士級-專任助理人員：陳玉洚
博士班研究生-兼任助理人員：李錦裳

報 告 附 件 ： 出席國際會議研究心得報告及發表論文

處 理 方 式 ：
1.公開資訊：本計畫可公開查詢
2.「本研究」是否已有嚴重損及公共利益之發現：否
3.「本報告」是否建議提供政府單位施政參考：否

中 華 民 國 103 年 10 月 31 日

中 文 摘 要 ： 抽菸會增加罹患心血管疾病的風險，並且經由發炎和氧化壓力引起傷害。肌動蛋白細胞骨架是一反應發炎刺激的關鍵演員，也是細胞內氧化壓力的早期攻擊目標。 本研究旨在探討人類EA.hy926內皮細胞在香菸煙霧提取物（cigarette smoke extract /CSE）刺激下，肌動蛋白細胞骨架的動態性變化。細胞免疫染色顯示CSE曝露導致劑量-及時間-依賴型肌動蛋白細胞骨架改造，並導致細胞皺縮。除此之外，細胞內鈣離子濃度也因CSE處理而明顯增高。以抗氧化劑(硫辛酸、谷胱乾甘肽，N-乙醯半胱氨酸、氨基胍、α-生育酚和維生素C)，鈣離子螯合劑（EGTA、BAPTA-AM）及一種強力的鈣池調控鈣離子通道（Store-operated Ca2+ channel/SOC)抑制劑（MRS-1845)前處理，均可明顯減低CSE所誘導之細胞內鈣離子變化及肌動蛋白細胞骨架重組和細胞形態的變化。此外，CSE誘導之細胞內鈣離子的增加，都可被三磷酸肌醇受體(inositol 1, 4, 5-trisphosphate receptor）抑制劑xestospongin C、磷脂酶C（phosphalipase C)抑制劑U-73122和蛋白激酶C（Protein kinase C）抑制劑GF109203X的前處理抑制，這些結果說明：活性氧物種(reactive oxygen species)的產生與細胞內鈣離子濃度增加，透過PLC/IP3/PKC的訊號通路在CSE 誘發的肌動蛋白解體和細胞皺縮扮演必要之角色。

中文關鍵詞： 香菸煙霧提取物、人類EA.hy926內皮細胞、肌動蛋白細胞骨架重組、鈣離子訊號、蛋白激酶 C、磷脂酶C、三磷酸肌醇受體

英 文 摘 要 ： Smoking increases the risk of cardiovascular disorders and leads to damage caused by inflammation and oxidative stress. The actin cytoskeleton is a key player in the response to inflammatory stimuli and is an early target of cellular oxidative stress. The purpose of this study was to investigate the changes in actin cytoskeleton dynamics in human endothelial EA.hy926 cells exposed to cigarette smoke extract (CSE). Immunostaining revealed that CSE exposure resulted in modification of the actin cytoskeleton and led to cell shrinkage in a dose- and time-dependent manner. In addition, the intracellular calcium concentration was increased by treatment with CSE. Pretreatment with antioxidants (lipoic acid, glutathione, N-acetyl cysteine, aminoguanidine, α-tocopherol, and vitamin C) significantly attenuated

the CSE-induced actin cytoskeleton reorganization and cell shrinkage. Calcium ion chelators (EGTA, BAPTA-AM AM) and a potent store-operated calcium channel (SOC) inhibitor (MRS 1845) also reduced CSE-induced intracellular calcium changes and attenuated actin cytoskeleton reorganization and cell morphology change. Moreover, the CSE-induced intracellular calcium increase was suppressed by pretreatment with the inositol trisphosphate receptor (IP3R) inhibitor xestospongin C, the phospholipase C (PLC) inhibitor U-73122, and the protein kinase C (PKC) inhibitor GF109203X. These results suggest that reactive oxygen species production and intracellular calcium increase play an essential role in CSE-induced actin disorganization and cell shrinkage through a PLC-IP3-PKC signaling pathway.

英文關鍵詞： cigarette smoke extract, human endothelial EA.hy926 cells, actin cytoskeleton reorganization, calcium signal, protein kinase C, phospholipase C, inositol trisphosphate receptor

科技部補助專題研究計畫成果報告

（□期中進度報告/■期末報告）

香菸煙霧水提取物造成人類血管內皮細胞及斑馬魚幼蟲發炎特性及保健防治研究

計畫類別：■個別型計畫　□整合型計畫

計畫編號：MOST 101－2320－B－040－019－MY2

執行期間：101年 08月 01日至 103年 07月 31日

執行機構及系所：中山醫學大學-生物醫學科學學系

計畫主持人：王祖興

共同主持人：

計畫參與人員：陳玉洚、李錦裳

本計畫除繳交成果報告外，另含下列出國報告，共 _1_ 份：

□執行國際合作與移地研究心得報告

■出席國際學術會議心得報告

期末報告處理方式：

1. 公開方式：

■非列管計畫亦不具下列情形，立即公開查詢

□涉及專利或其他智慧財產權，□一年□二年後可公開查詢

2.「本研究」是否已有嚴重損及公共利益之發現：□否 □是

3.「本報告」是否建議提供政府單位施政參考 □否 □是，____（請列舉提供之單位；本部不經審議，依勾選逕予轉送）

中　華　民　國　103 年 10 月 31 日

目錄

中文摘要

抽菸會增加罹患心血管疾病的風險，並且經由發炎和氧化壓力引起傷害。肌動蛋白細胞骨架是一反應發炎刺激的關鍵演員，也是細胞內氧化壓力的早期攻擊目標。 本研究旨在探討人類 EA.hy926 內皮細胞在香菸煙霧提取物（cigarette smoke extract /CSE）刺激下，肌動蛋白細胞骨架的動態性變化。細胞免疫染色顯示 CSE 曝露導致劑量-及時間-依賴型肌動蛋白細胞骨架改造，並導致細胞皺縮。除此之外，細胞內鈣離子濃度也因 CSE 處理而明顯增高。以抗氧化劑(硫辛酸、谷胱乾甘肽，*N*-乙醯半胱氨酸、氨基胍、α-生育酚和維生素 C)，鈣離子螯合劑（EGTA、BAPTA-AM）及一種強力的鈣池調控鈣離子通道（Store-operated Ca^{2+} channel/SOC)抑制劑 (MRS-1845)前處理，均可明顯減低 CSE 所誘導之細胞內鈣離子變化及肌動蛋白細胞骨架重組和細胞形態的變化。此外，CSE 誘導之細胞內鈣離子的增加，都可被三磷酸肌醇受體(inositol 1, 4, 5-trisphosphate receptor）抑制劑 xestospongin C、磷脂酶 C（phosphalipase C)抑制劑 U-73122 和蛋白激酶 C（Protein kinase C）抑制劑 GF109203X 的前處理抑制，這些結果說明：活性氧物種(reactive oxygen species)的產生與細胞內鈣離子濃度增加，透過 PLC/IP3/PKC 的訊號通路在 CSE 誘發的肌動蛋白解體和細胞皺縮扮演必要之角色。

關鍵字： 香菸煙霧提取物、人類 EA.hy926 內皮細胞、肌動蛋白細胞骨架重組、鈣離子訊號、蛋白激酶 C、磷脂酶 C、三磷酸肌醇受體

英文摘要

Smoking increases the risk of cardiovascular disorders and leads to damage caused by inflammation and oxidative stress. The actin cytoskeleton is a key player in the response to inflammatory stimuli and is an early target of cellular oxidative stress. The purpose of this study was to investigate the changes in actin cytoskeleton dynamics in human endothelial EA.hy926 cells exposed to cigarette smoke extract (CSE). Immunostaining revealed that CSE exposure resulted in modification of the actin cytoskeleton and led to cell shrinkage in a dose- and time-dependent manner. In addition, the intracellular calcium concentration was increased by treatment with CSE. Pretreatment with antioxidants (lipoic acid, glutathione, *N*-acetyl cysteine, aminoguanidine, α-tocopherol, and vitamin C) significantly attenuated the CSE-induced actin cytoskeleton reorganization and cell shrinkage. Calcium ion chelators (EGTA, BAPTA-AM AM) and a potent store-operated calcium channel (SOC) inhibitor (MRS 1845) also reduced CSE-induced intracellular calcium changes and attenuated actin cytoskeleton reorganization and cell morphology change. Moreover, the CSE-induced intracellular calcium increase was suppressed by pretreatment with the inositol trisphosphate receptor (IP3R) inhibitor xestospongin C, the phospholipase C (PLC) inhibitor U-73122, and the protein kinase C (PKC) inhibitor GF109203X. These results suggest that reactive oxygen species production and intracellular calcium increase play an essential role in CSE-induced actin disorganization and cell shrinkage through a PLC-IP3-PKC signaling pathway.

Keywords: cigarette smoke extract, human endothelial EA.hy926 cells, actin cytoskeleton reorganization, calcium signal, protein kinase C, phospholipase C, inositol trisphosphate receptor

INTRODUCTION

Cigarette smoking harms nearly every organ in the body, including the heart, blood vessels, lungs, eyes, mouth, reproductive organs, bones, bladder, and digestive organs. Smoking is recognized as a risk factor for cardiovascular disorder, chronic obstructive pulmonary disease, type 2 diabetes, Alzheimer's disease and cancers (particularly lung cancer, cancers of the larynx and mouth, and pancreatic cancer) (Kuper et al., 2002; Yoshida & Tuder, 2007; Xie et al., 2009; Cataldo et al., 2010; Matsuo et al., 2011; Breitling, 2013). Cigarette smoke is a complex mixture of more than 7000 chemicals, most of which are known toxicants and carcinogens (USDHHS, 2010). Although the mechanisms responsible are not fully clear, oxidative stress plays a central and common role in the development of smoking-related diseases. In fact, cigarette smoke itself contains high levels of reactive oxygen species (ROS), reactive nitrogen species (RNS), and reactive carbon species (RCS) (Bartalis et al., 2009; Yu et al., 2012).Many previous reports also have shown that exposure to cigarette smoke extract (CSE) potently induces the generation of ROS and RNS in different cell types (Valavanidis et al., 2009). The increase in oxidative stress subsequently leads to multiple cellular injuries. Our previous and other studies have shown that exposure to CSE quickly induces ROS-dependent DNA damage and cell shrinkage and reorganization of the actin cytoskeleton in human endothelial cells (Bernhard et al., 2003; Chen et al., 2004; Schweitzer et al., 2011; Gagat et al., 2013; Kim et al., 2013). Recently, we further reported that reorganization of the actin cytoskeleton is partially involved in the CSE-induced expression of intercellular adhesion molecule 1 (ICAM-1) in human endothelial cells (Chen et al., 2009). These findings highlight the importance of actin dynamics in smoke-induced endothelial barrier dysfunction and pre-inflammatory gene expression changes in human vascular endothelium.

Intracellular calcium homeostasis is well known to act as a determining factor in numerous cellular responses, including cell motility, gene transcription, muscle contraction, exocytosis, and cell death (Berridge et al. 2003; Harr and Distelhorst, 2010). Calcium homeostasis is tightly controlled by various calcium-transporting proteins, including calcium-permeable ion channels. These calcium-permeable channels include transient receptor potential channels (TRPCs), store-operated calcium channels (SOCs), voltage-gated calcium channels, two-pore channels, mitochondrial permeability transition pore, mitochondrial calcium uniporter, inositol trisphosphate (IP3) and ryanodine receptors, and others. These channels contribute to changes in $[Ca^{2+}]_i$ by providing pathways for Ca^{2+} entry, by modulating the driving force for the Ca^{2+} entry, and by providing intracellular pathways for Ca^{2+} uptake and release to and from cellular organelles (Pedersen et al., 2005; Bernardi and von Stockum, 2012; Rizzuto et al., 2012).

A close relationship exists between intracellular Ca^{2+} mobilization and microfilament rearrangement in mammalian cell lines. Disruption of microfilaments activates membrane calcium-permeable channels and increases intracellular calcium concentrations in different cell lines (Rivas et al., 2004; Babich and Burkhardt, 2013; Wu et al., 2013). Many key proteins involved in the regulation of actin dynamics are also Ca^{2+}-sensitive. These include proteins such as the gelsolin family of actin-binding proteins, which are regulated directly by Ca^{2+}, as well as proteins like talin, ezrin, and WASp, which are sensitive to cleavage by Ca^{2+}-dependent calpain (Babich & Burkhardt, 2013; Jeong et al., 2013). However, it is unknown whether exposure to CSE causes a sustained increase in the intracellular calcium signal and reorganization of the actin cytoskeleton, which ultimately up-regulates the expression of the many proinflammatory genes, including ICAM-1. Therefore, the purpose of this study was to investigate the possible mechanism by which reorganization of the

actin cytoskeleton is initiated by CSE exposure in human endothelial EA.hy926 cells, especially the calcium-related signaling pathways involved.

MATERIALS AND METHODS

Chemicals

Cell culture reagents (DMEM, penicillin, streptomycin, and fetal bovine serum) were obtained from Gibco Laboratories (Grand Island, NY). Chemicals were of the purest analytical grade. BAPTA-AM AM, EGTA, MRS 1845, and GF109203X were from Tocris Bioscience (Ellisville, MO). Fluo-3 AM was obtained from Biotium (Hayward, CA). Rhodamine-phalloin was obtained from Molecular Probes (Eugene, OR), and all other chemicals were from Sigma Chemical Co. (St. Louis, MO).

Preparation of the Cigarette Smoke Extract

A nonfractionated CSE was prepared as described (Chen et al., 2004). Commercial filter-tipped cigarettes (Marlboro; Philip Morris Inc., Richmond, VA) were smoked continuously in the apparatus designed by Su et al. (1998). Mainstream smoke was forced through 15 ml of phosphate-buffered saline (PBS) by the application of a water pump vacuum. Each cigarette was smoked for 5 min, and three cigarettes were used per 15 ml of PBS to generate a CSE solution. The CSE solution was diluted with culture medium and used immediately. Final concentrations of these solutions are expressed as percentage values.

Cell Culture

The human endothelial cell line EA.hy926 (ATCC: CRL-2922) was originally derived from human umbilical vein and shows vascular endothelial cell characteristics. EA.hy926 cells were cultured in DMEM culture medium supplemented with 10% fetal bovine serum, 100 units/mL penicillin, and 100 μg/mL streptomycin at 37°C in a humidified atmosphere of 5% CO_2.

CSE Treatment of Cells

In this study, Ea.hy926 cells were treated with CSE in two different ways. Stand-alone treatment: Cells were treated with different concentrations of CSE (0%, 1%, 2.5%, 5% or 10%) in complete medium for hours indicated. After treatment the cell shape change and calcium ion concentration were analyzed by rhodamine-phalloidin stains and Ca^{2+}-sensititive fluorochrome Fluo-3/acetoxymethyl ester (Fluo-3/AM) staining, respectively. Combined treatment: an antioxidant, signal transduction inhibitor or calcium chelator was added 30 minutes before CSE treatment in complete medium for hours indicated. All cultures were performed in complete BMEM medium, except for the combination treatment of BAPTA-AM and CSE was done in a calcium-free medium.

Fluo-3 AM Staining Microscopy

For detection of intracellular Ca^{2+}, epi-fluorescence microscopy was conducted by following previous studies (Wang et al., 2011). The dye Fluo-3 AM ester (Fluo-3 AM) was used in the staining by following the supplier's instructions. Briefly, Fluo-3 AM was dissolved in DMSO at a concentration of 5 mM. After treatment, cells were washed once with PBS and loaded with 2 mM Fluo-3 AM for 30 min in a cell incubator. After incubation, cells were washed once with PBS to remove the probes and cultured in 1x PBS for another 30 minutes to allow complete de-esterification of intracellular Fluo-3 AM. Cells were then washed once with PBS and the samples were covered with mounting medium and a coverslip. Samples were finally observed through a AxioSkop 2 Plus microscope (Zeiss, Jena, Germany) and the images were detected and analyzed by using Image J software. (NIH, Bethesda, MD)

Staining for Actin Cytoskeleton

EA.hy926 cells were plated at a density of 5×10^4 cells/well in a 4-well chamber slide, and after overnight culture, cells were treated with different concentrations of CSE for hours indicated. After CSE treatment, cells were fixed with 3.7% paraformaldehyde (v/v) in PBS for 15 min and permeabilized with 0.1% Triton X-100 in PBS for 5 min at room temperature. To stain F-actin, cells were incubated with rhodamine-phalloidin for 30 min. Nuclei were stained with 1 mg/mL diamidino-2-phenylindole dihydrochloride for 10 min. The slides were mounted with Dako anti-fade mounting media. The actin cytoskeleton and nuclei were observed under a fluorescence microscope.

Fluorescence Measurements of F-actin Formation

For determination of F-actin content after incubation, test reagents were added to the cell incubation buffer and incubation was continued for various periods of time (as defined for individual experiments) after which the medium was removed. The F-actin content of the cells was then determined by a method based on that described by Wu et al. (1992) for chromaffin cells. Cells were fixed by the addition of 0.3 mL of 3.7% formaldehyde in PBS and were incubated for 15 min at room temperature. An aliquot (0.3 mL) of Triton X-100 (0.20% in PBS) was then added to permeabilize the cells, after which 0.3 mL of rhodamine-phalloidin (1.5 μM in PBS) was added and left for 5 min. The cells were washed three times with 1 mL PBS each and dissolved in 1 mL of 0.1 M NaOH. Fluorescence of the samples was measured by using a model F-4500 (Hitachi Co., Ltd., Tokyo, Japan) with excitation and emission wavelengths of 540 nm and 560 nm, respectively.

Cell Spreading Assay

Cells were seeded into a 24-well plate at a density of 1×10^5 cells per well and were fixed at the indicated time point. Spread and non-spread cells were counted in five representative high-power fields. Poor-spread cells were defined as small, round cells with little or no membrane protrusions, whereas spread cells were defined as large cells with extensive protrusion of broad lamellipodia and elongated filopodia. The results represent the percentage of well-spread cells in five random high-power fields. More than 100 cells were analyzed per sample. The data are presented as the average of the results from three independent experiments.

Statistical Analysis

Data are expressed as the mean ± S.E. from at least three independent experiments. Statistical analysis was performed with commercially available software (SAS Institute Inc., Cary, NC). Data were analyzed by one-way ANOVA and Tukey's multiple comparison test. A value of $P < 0.05$ was considered to be significant.

RESULTS

CSE Induced Changes in Cell Morphology and the Actin Cytoskeleton

Treatment with CSE changed the cell morphology from a well-spread to a shrunken and rounded shape and disrupted the actin cytoskeleton networks in a dose-dependent manner (Fig. 1A). Next, cells were analyzed for phalloidin intensity integrated over the entire cell area to determine a relative level of F-actin assembly weighted by the cell size (measured as intensity arbitrary unit x μm^2). As shown in Fig. 1B, CSE exposure dose-dependently decreased the relative level of cellular F-actin assembly. To evaluate the time-course effect of CSE on both the decrease in the proportion of well-spread cells and the relative cellular level of F-actin assembly, EA.hy926 cells were exposed to CSE for up to 4 hours. A decreased proportion of well-spread cells and a decrease in the relative cellular level of F-actin assembly were rapidly induced 1 hour after exposure to 5% CSE (Figs. 2A & 2B). Prolonging the CSE exposure time to 2 or 4 hours did not further reduce the proportion of well-spread cells or the relative level of F-actin assembly.

Oxidative Stress and CSE Induced Changes in Cell Morphology and the Actin Cytoskeleton

To further investigate whether oxidative stress was involved in the CSE-induced F-actin reorganization and cell shrinkage, cells were pretreated with various antioxidants for 30 minutes and then co-treated with 10% CSE for another 4 hours. The percentage of well-spread cells and the levels of F-actin were evaluated by fluorescence microscopy after labeling with rhodamine-phalloidin. The results showed that thiol-containing antioxidants, such as *N*-acetyl cysteine, glutathione, and lipoic acid, significantly prevented the CSE-induced decrease in the fraction of well-spread cells (Fig. 3). The maximum percent recovery of *N*-acetyl cysteine, glutathione, and lipoic acid on the CSE-induced decrease in well-spread cells were 80.9% at 10 mM, 89.4% at 5 mM, and 74.1% at 25 mM, respectively. Protection by non-thiol-containing antioxidants, including vitamin C, alpha-tocopherol, and aminoguanidine, was examined as well. These results showed that non-thiol-containing antioxidants provided 20% less protection than did thiol-containing antioxidants against the CSE-induced decrease in the fraction of well-spread cells (Fig. 4). The maximum percent recovery was 66.4% at 100 μM vitamin C, 58.8% at 25 μM alpha-tocopherol, and 70% at 15 mM aminoguanidine. These findings clearly suggest that the decrease in the fraction of well-spread cells induced by CSE is a ROS-dependent stress response.

Calcium Signaling and CSE Induced Changes in Cell Morphology and the Actin Cytoskeleton

Changes in intracellular calcium signaling are also a key factor in actin dynamics and cell spreading. To determine whether calcium ion signaling was involved in the CSE-induced decrease in well-spread cells, we added calcium chelators 30 minutes before exposure to CSE for 4 hours and then determined cell spreading by staining with rhodamine-phalloidin after treatment. The results showed that BAPTA-AM AM as well as EGTA dose-dependently reduced the CSE-induced morphology changes. The maximum percent recovery was 91.1% for 50 μM EGTA and 68.4% for 5 μM BAPTA-AM AM, respectively (Figs. 5A & 5B). In addition, the CSE-induced loss of well-spread cells was suppressed by the store-operated Ca^{2+} entry (SOCE) inhibitor

MRS 1845 (Fig. 5C). Collectively, these findings suggested that elevation of the intracellular Ca^{2+} concentration through both extracellular Ca^{2+} influx via TRP-related cation channels and Ca^{2+} release from intracellular stores are related to the CSE-induced F-actin reorganization and loss of well-spread cells.

To further verify that a sustained elevation of intracellular calcium ion was necessary for the CSE-induced decrease in well-spread cells, was assessed changes in the intracellular free Ca^{2+} concentration of CSE-treated EA.hy926 cells by use of Fluo3-AM. The results clearly showed that, after an 8-hour treatment, CSE (2.5%, 5%, and 10%) dose-dependently increased the intracellular Ca^{2+}concentration (Fig. 6). The fold induction of intracellular Ca^{2+} by CSE was 1.6-, 2.5-, and 2.8-fold for 2.5%, 5%, and 10% CSE, respectively. In the presence of BAPTA-AM AM and EGTA, the CSE-induced elevation in Ca^{2+} was apparently attenuated (Figs. 7A & 7B). The SOCE blocker MRS1845 also inhibited the CSE-induced elevation of intracellular Ca^{2+}, but to a lesser extent than that noted by calcium chelators (Fig. 7C). The data presented herein indicate that both release of calcium from an intracellular source and influx of extracellular are major contributors to the calcium elevation induced by CSE in human endothelial cells. TRPCs, however, may play only a partial role in the increase in calcium influx induced by CSE.

Calcium Signaling Pathway and CSE Induced Changes in Cell Morphology and the Actin Cytoskeleton

Several lines of evidence suggest that activation of receptors coupled to the phospholipase C/IP3 signaling pathway results in a rapid release of calcium from its intracellular stores, eventually leading to depletion of these stores. Calcium store depletion triggers an influx of extracellular calcium across the plasma membrane. To examine whether PLC and IP_3R activation are involved in this CSE-induced elevation of intracellular calcium in EA.hy926 cells, the effects of the phospholipase C inhibitor U-73122 and the IP3R inhibitor XeC (xestospongin C) were determined. As shown, the CSE-induced increase in intracellular calcium was blocked by U-73122 in a dose-dependent manner (Fig. 8A). In the presence of XeC, the CSE-triggered elevation in intracellular calcium in EA.hy926 cells was also dose-dependently reduced (Fig. 8B).

In addition to the PLC/IP3R signaling, a broad inhibitor of PKC isoforms, GF109203X, also completely inhibited the CSE-induced intracellular calcium elevation (Fig. 8C). This finding indicated that PKC activation was one of the key factors in the regulation of the CSE-induced Ca^{2+} release from intracellular stores and the Ca^{2+} influx from the extracellular space. The concentration-dependent effects of calcium signal modulators on CSE-induced Ca^{2+} concentration elevation were summarized in Table 1. On the other hand, the L-type voltage-gated calcium channel blocker nifedipine did not affect CSE-induced calcium elevation (data not shown).

DISCUSSION

In the present study, we have shown that CSE induces cell damage by changing (or disrupting) the organization of the actin cytoskeleton through ROS-dependent calcium signaling. An integrated working model of the CSE-induced elevation of intracellular Ca^{2+} ions and cell shrinkage is proposed in Fig. 9. First, CSE exposure causes lipid oxidation and endoplasmic reticulum stress through oxidative stress. Second, CSE-induced lipid peroxidation products activate phospholipase C and form IP3, which activates IP3 receptors (IP3Rs) to induce Ca^{2+} release from IP3-sensitive endoplasmic reticulum stores. The rise in intracellular Ca^{2+} may induce F-actin reorganization and activate conventional or novel PKCs alone or in combination with diacylglycerol derived from PLC digestion. Upon activation, PKC is translocated to the plasma membrane where it stimulates opening of TRPCs and SOCs as the result of protein phosphorylation. The opening of SOCs on the plasma membrane results in calcium influx. Finally, the CSE-induced elevation of the intracellular calcium ion concentration alone or together with ROS production causes marked F-actin cytoskeletal disorganization and cell shrinkage.

Previous reports have shown that CSE exposure induces an increase in cytosolic or mitochondrial ROS production in various types of cells, includingbrain and pulmonary endothelial cells (Shih et al., 2011; Kim et al., 2013; Rasmussen et al., 2014) . In fact, cigarette smoke is known to contain a large number of oxidants. Moreover, CSE has been shown to cause lipid peroxide products, such as 4-hydroxy-2-nonenal, malondialdehyde, acrolein, and acetaldehyde, either directly or indirectly from endogenous sources in various cell types in vitro and in vivo (Rainey et al., 2009; Nagamma et al., 2011). These findings indicate that cigarette smoke or CSE is a universal and potent inducer of ROS in mammalian cells. Although the component(s) responsible for CSE-induced intracellular ROS production remain unclear, CSE-induced ROS production may originate from at least three primary sources: activation of cytosolic NADPH oxidase (Jaimes et al., 2004), activation of xanthine oxidase (Kim et al., 2013), and mitochondrial dysfunction (van der Toorn et al., 2009). This explains why antioxidant supplements reduce different cigarette smoke- or CSE-induced types of cell injury, especially genotoxicity and oxidative stress in vitro and in vivo (Tsuda et al., 2000; Chen et al., 2004; Messier et al., 2013). In this study, the effectiveness of a variety of antioxidants for preventing CSE-induced F-actin disruption and cell shrinkage (Figs. 3 and 4) suggests that the initial ROS production acts as a key mediator in cell injury induced by cigarette smoke.

Actin is known to be a major target of ROS attack under oxidative stress. In the resulting modification, a carbonyl (C = O) group is introduced into the actin molecule (Castro et al., 2013). Actin carbonylation causes the formation of protein aggregates, disrupts the actin cytoskeleton, and leads to the loss of the monolayer barrier function (Dalle-Donne et al., 2001). Reactive carbonyl species can be derived from exposure to CSE and the oxidation of lipids (acrolein, 4-hydroxynonenal, malondialdehyde) and sugars (glyoxal, methylglyoxal) (Suzuki et al., 2010). Although it was not determined in this study, an increase in actin carbonylation by CSE was reported in our previous work (Lin et al., 2009) and in a recent report by Gornati et al. (2013). In the present study, CSE-induced actin disorganization and cellular shrinkage were effectively prevented by various antioxidants, including *N*-acetyl cysteine, glutathione, lipoic acid, vitamin C, vitamin E, and aminoguanidine (Figs. 3 and 4). These results also indirectly indicate that ROS production is involved in CSE-induced actin disorganization and cellular shrinkage.

Glutathione, *N*-acetyl cysteine, and lipoic acid are potent thiol-containing free radicals, aldehydes, and metals scavengers (Biewenga et al., 1997; Galano, 2011; Matsufuji et al., 2013). Cigarette smoke and CSE are

rich source of ROS, reactive nitrogen species, and aldehydes, which have pathological effects (van der Toorn et al., 2013; Lu et al., 2003; Pryor & Stone, 1993). For instance, α,β-unsaturated aldehydes released by cigarette smoke actively attack actin molecules by carbonylation modification (Aldini et al., 2007; Dalle-Donne et al., 2007). Carbonylated actin disrupts the actin cytoskeleton and results in a loss of barrier function in human colonic cells exposed to hypochlorous acid (Dalle-Donne et al., 2001). The aldehydes produced in cigarette smoke have also been demonstrated to play a critical role in inflammatory responses (van der Toorn et al., 2013; Andrè et al., 2008). On the basis of this evidence, we can conclude that damage to the actin cytoskeleton by cigarette smoke is closely related to the increase in ROS- and aldehyde-mediated carbonyl stress.

Oxidative stress increases the intracellular Ca^{2+} concentration (Quintanar-Escorza et al., 2010) and activates Ca^{2+}-dependent signaling that participates in the regulation and integration of diverse cellular functions (Nunes & Demaurex, 2014; Mazars et al., 2010). In the present study, the intracellular Ca^{2+} level was dose-dependently increased by CSE (Fig. 6) and this increase was attenuated by either a cell-membrane-permeable (BAPTA-AM AM) (Fig. 7A) or a cell-membrane-impermeable (EGTA) calcium chelator (Fig. 7B) and also by the SOCE inhibitor MRS-1845 (Fig. 7C). These results suggested that the CSE-induced calcium ion elevation was due to both release of Ca^{2+} from internal stores and influx of extracellular Ca^{2+}.

Several recent studies have provided conclusive evidence that Orai1- and TRPC1-mediated SOCE are an important means of Ca^{2+} entry in endothelial cells (Tiruppathi et al., 2006, Yao & Garland, 2005; Derler et al., 2012). Additionally, TRPC1 was shown to interact with cytoskeletal modulators such as RhoA, which suggests that local cytoskeletal rearrangements might be associated with the TRPC1 regulation of SOCE (Galán et al., 2011; Mehta et al., 2003). Reorganization of the actin cytoskeleton has also been shown to modulate the functional interaction between TRPC1 and its main molecular components, such as IP3R, STIM-1, and Orai1, and subsequent activation of SOCE in mammalian cells (Jardin et al., 2008; Galán et al., 2011). Inhibition of actin dynamics blocks the activation of TRPC1 induced by stretching and thapsigargin (an inducer of stored Ca^{2+} release) (Vanoverberghe et al., 2012; Formigli et al., 2009; Mehta et al., 2003). Furthermore, it has been shown that rapid actin depolymerization requires cofilin dephosphorylation and that SOCE is activated by conformational coupling of the type 2 inositol 1,4,5-trisphosphate receptor (IP3RII) to hTRPC1 (Redondo et al., 2006). Collectively, these results show that actin reorganization is necessary for the activation of SOCE in mammalian cells. Early actin disruption not only removes the physical barrier, but also provides a possibility for the formation of a macromolecular store-dependent complex required for the activation and regulation of SOCE. The molecular components of this macromolecular store-dependent complex may contain STIM1, Orai1, TRPCs, and other regulatory proteins, such as caveolin-1, phospholipase C, and protein kinase C. Nevertheless, the molecular mechanisms responsible for CSE-induced actin reorganization and its role in SOCE activation will require further investigation to be defined in human endothelial cells.

Although the PLC-PKC cascade is a key signaling pathway involved in SOCE in different cell types (Sabourin et al., 2012; Antigny et al., 2011), little is known about this signaling pathway in cigarette smoke-induced Ca^{2+} mobilization and actin cytoskeleton disarrangement in human cells. PLC cleaves the phospholipid phosphatidylinositol 4,5-bisphosphate (PIP_2) into diacylglycerol and IP3. This high local concentration of IP3 diffuses away and activates its receptor (IP_3R). Alternatively, it seems that the activation

of IP3R can also be mediated by reorganization of the actin cytoskeleton to facilitate the localization of PLC close to the IP3R. These events result in an increase in the cytosolic Ca^{2+} concentration, causing a cascade of intracellular changes and activity. Furthermore, Ca^{2+} and diacylglycerol together activate conventional PKCs. PKC can exert inhibitory or stimulatory effects on SOCE depending on cell types and their isoforms (Gao et al., 2012; Kawasaki et al., 2010). Moreover, PKC has been shown to activate the function of TRPC3 in B cells and myocytes (Poteser et al., 2011; Numaga et al., 2010). Besides TRPC3, TRPC1 channel activity is also regulated by PKC-dependent phosphorylation (Saleh et al., 2009). In human endothelial cells, TRPC1 has shown to be directly phosphorylated by PKC-α (Ahmmed et al., 2004). Previous reports have also shown that cigarette smoke activates different PKC isoforms in different cell types, including PKC-*α* and -*ε in* rat C6 glioma cells (Mai et al., 2012); PKC-α, -ζ, -ε, and -η in human lung fibroblasts (Park et al., 2008); and PKC-ε, -η, and -θ in rat bronchial smooth muscle cells (Ye et al., 2008). The results of the present study clearly showed that the CSE-induced intracellular Ca^{2+} increase was effectively blocked by the PLC inhibitor U-73122 and the PKC inhibitor GF109203X (Fig. 8), which suggests that the PLC-PKC pathway plays an important role in this action. As stated above, various PKC isoforms are associated with cellular Ca^{2+} homeostasis, and further study is required to ascertain which isoforms may be functionally involved in CSE-induced calcium mobilization, F-actin disorganization, and cell shrinkage. Moreover, it should be noted that our findings were inconsistent with a recent study in which reported that vapor phase cigarette smoke induced an IP3-independent release of calcium from lysosome in four different cell lines (Rasmussen et al., 2014). These inconsistent results may be due to variable such as differences in cigarette smoke preparation and cell type specificity. In fact, previous report has demonstrated that CSE exposure has differential effects on the lings and tracheal epithelium compared to vapor phase cigarette smoke exposure has (Elliott et al., 2006).

In conclusion, the findings of this study demonstrate that, in human endothelial cells, CSE exposure induces a sustained elevation of intracellular calcium, likely through the PLC/IP3/PKC signaling pathway, which activates a calcium signal. Elevation of intracellular ROS and Ca^{2+} levels induced by CSE leads to actin cytoskeleton reorganization and cell shrinkage. These phenomena indicate that cigarette smoke has high potential to destroy the barrier function of the endothelial monolayer and to increase the risk of vascular disorders in smokers. Calcium supplementation of smokers must be done carefully and be appropriately monitored.

ACKNOWLEDGMENTS

This study was supported by a grant from the National Science Council, ROC (NSC 101-2320-B-040-019-MY2).

Table 1. Summary of the inhibitory effects of calcium signaling modulators on CSE-induced calcium ion elevation in human EA.hy926 endothelial cells.

Modulators	Percent inhibition[1]
BABTA	
5.0 μM	67.8 ± 12.8
10.0 μM	80.9 ± 12.6
EGTA	
1.0 mM	57.1 ± 10.1
2.0 mM	78.5 ± 14.8
MRS 1845	
5.0 μM	32.1 ± 12.8
10.0 μM	36.9 ± 10.1
GF109203X	
0.5 μM	28.9 ± 10.5
1.0 μM	83.3 ± 9.6*
U-73122	
2.5 μM	33.3 ± 11.0
5.0 μM	91.6 ± 4.1**
Xestospongin C (XeC)	
5.0 μM	19.4 ± 2.7
10.0 μM	48.6 ± 8.4

[1]Percent inhibition (I%)was calculated by the following formula: I% = [1- (fluorescence intensity of fluo-3 in cells treated with calcium modulator and 5% CSE – fluorescence intensity of fluo-3in cells treated with 5% CSE] / (fluorescence intensity of fluo-3 in cells treated with 5% CSE – fluorescence intensity of fluo-3 in untreated control cells)] x 100%.

REFERENCES

Ahmmed GU, Mehta D, Vogel S, Holinstat M, Paria BC, Tiruppathi C, Malik AB. 2004. Protein kinase Calpha phosphorylates the TRPC1 channel and regulates store-operated Ca2+ entry in endothelial cells. J Biol Chem 279: 20941-20949.

Aldini G, Orioli M, Carini M. 2007. Alpha,beta-unsaturated aldehydes adducts to actin and albumin as potential biomarkers of carbonylation damage. Redox Rep 12: 20-25.

Andrè E, Campi B, Materazzi S, Trevisani M, Amadesi S, Massi D, Creminon C, Vaksman N, Nassini R, Civelli M, Baraldi PG, Poole DP, Bunnett NW, Geppetti P, Patacchini R. 2008. Cigarette smoke-induced neurogenic inflammation is mediated by alpha,beta-unsaturated aldehydes and the TRPA1 receptor in rodents. J Clin Invest 118: 2574-2582.

Babich A, Burkhardt JK. 2013. Coordinate control of cytoskeletal remodeling and calcium mobilization during T-cell activation. Immunol Rev 256: 80-94.

Bartalis J, Zhao YL, Flora JW, Paine JB, Wooten JB. 2009. Carbon-centered radicals in cigarette smoke: acyl and alkylaminocarbonyl radicals. Anal Chem 81: 631-641.

Bernardi P, von Stockum S. 2012. The permeability transition pore as a Ca(2+) release channel: new answers to an old question. Cell Calcium 52: 22-27.

Bernhard D, Pfister G, Huck CW, Kind M, Salvenmoser W, Bonn GK, Wick G. 2003. Disruption of vascular endothelial homeostasis by tobacco smoke: impact on atherosclerosis. FASEB J l17: 2302-2304.

Berridge MJ, Bootman MD, Roderick HL. 2003. Calcium signalling: dynamics, homeostasis and remodelling. Nat Rev Mol Cell Biol 4: 517-529.

Biewenga GP, Haenen GR, Bast A. 1997. The pharmacology of the antioxidant lipoic acid. Gen Pharmacol 29: 315-331.

Breitling LP. 2013. Current genetics and epigenetics of smoking/tobacco-related cardiovascular disease. Arterioscler Thromb Vasc Biol. 33: 1468-1472.

Castro JP, Jung T, Grune T, Almeida H. 2013. Actin carbonylation: from cell dysfunction to organism disorder. J Proteomics 92:171-180.

Cataldo JK, Prochaska JJ, Glantz SA. 2010. Cigarette smoking is a risk factor for Alzheimer's Disease: an analysis controlling for tobacco industry affiliation. J Alzheimers Dis 19:465-480.

Chen HW, Chien ML, Chaung YH, Lii CK, Wang TS. 2004. Extracts from cigarette smoke induce DNA damage and cell adhesion molecule expression through different pathways. Chem Biol Interact 150:233-241.

Chen HW, Lii CK, Ku HJ, Wang TS. 2009. Cigarette smoke extract induces expression of cell adhesion molecules in HUVEC via actin filament reorganization. Environ Mol Mutagen 50:96-104.

Dalle-Donne I, Carini M, Vistoli G, Gamberoni L, Giustarini D, Colombo R, Maffei Facino R, Rossi R, Milzani A, Aldini G. 2007. Actin Cys374 as a nucleophilic target of alpha,beta-unsaturated aldehydes. Free Radic Biol Med 42:583-598.

Dalle-Donne I, Rossi R, Milzani A, Di Simplicio P, Colombo R. 2001 The actin cytoskeleton response to oxidants: from small heat shock protein phosphorylation to changes in the redox state of actin itself. Free Radic Biol Med 31: 1624-1632.

Derler I, Madl J, Schütz G, Romanin C. 2012. Structure, regulation and biophysics of I(CRAC), STIM/Orai1. Adv Exp Med Biol 740:383-410.

Elliott MK, Sisson JH, West WW, Wyatt TA. 2006. Differential in vivo effects of whole cigarette smoke exposure versus cigarette smoke extract on mouse ciliated tracheal epithelium. Exp Lung Res 32:99-118.

Formigli L, Sassoli C, Squecco R, Bini F, Martinesi M, Chellini F, Luciani G, Sbrana F, Zecchi-Orlandini S, Francini F, Meacci E. 2009. Regulation of transient receptor potential canonical channel 1 (TRPC1) by sphingosine 1-phosphate in C2C12 myoblasts and its relevance for a role of mechanotransduction in skeletal muscle differentiation. J Cell Sci 122:1322-1333.

Gagat M., Grzanka D., Izdebska M., Sroka W.D., Marszałł M.P., Grzanka A., 2013. Tropomyosin-1 protects endothelial cell-cell junctions against cigarette smoke extract through F-actin stabilization in EA.hy926 cell line. Acta Histochemica (in print).

Galán C, Dionisio N, Smani T, Salido GM, Rosado JA, 2011. The cytoskeleton plays a modulatory role in the association between STIM1 and the Ca2+ channel subunits Orai1 and TRPC1. Biochem Pharmacol 82:400-410.

Galano A, J. Raúl Alvarez-Idaboy JR. 2011. Glutathione: mechanism and kinetics of its non-enzymatic defense action against free radicals. RSC Adv 1:1763-1771

Gao Y, Zou J, Geng S, Zheng J, Yang J, 2012. Role of protein kinase C in the activation of store-operated Ca(2+) entry in airway smooth muscle cells. J Huazhong Univ Sci Technolog Med Sci 32:303-310.

Gornati R, Colombo G, Clerici M, Rossi F, Gagliano N, Riva C, Colombo R, Dalle-Donne I, Bernardini G, Milzani A. 2013. Protein carbonylation in human endothelial cells exposed to cigarette smoke extract. Toxicol Lett 218:118-128.

Harr MW, Distelhorst CW. 2010. Apoptosis and autophagy: decoding calcium signals that mediate life or death. Cold Spring Harb Perspect Biol 2:a005579.

Jaimes EA, DeMaster EG, Tian RX, Raij L. 2004. Stable compounds of cigarette smoke induce endothelial superoxide anion production via NADPH oxidase activation. Arterioscler Thromb Vasc Biol 24:1031-1036.

Jardin I, Salido GM, Rosado JA. 2008. Role of lipid rafts in the interaction between hTRPC1, Orai1 and STIM1. Channels (Austin) 2:401-403.

Jeong SY, Martchenko M, Cohen SN. 2013. Calpain-dependent cytoskeletal rearrangement exploited for anthrax toxin endocytosis. PNAS 110:E4007-E4015.

Kawasaki T, Ueyama T, Lange I, Feske S, Saito N. 2010. Protein kinase C-induced phosphorylation of Orai1 regulates the intracellular Ca2+ level via the store-operated Ca2+ channel. J Biol Chem 285:25720-25730.

Kim BS, Serebreni L, Hamdan O, Wang L, Parniani A, Sussan T. 2013. Scott Stephens R, Boyer L, Damarla M, Hassoun PM, Damico R. Xanthine oxidoreductase is a critical mediator of cigarette smoke-induced endothelial cell DNA damage and apoptosis. Free Radic Biol Med 60:336-346.

Kuper H, Boffetta P, Adami HO. 2002. Tobacco use and cancer causation: association by tumour type. J Intern Med 252:206-224.

Lin CC, Su TH, Wang TS. 2009. Protein carbonylation in THP-1 cells induced by cigarette smoke extract via a copper-catalyzed pathway. Chem Res Toxicol 22:1232-1238.

Lu X, Cai J, Kong H, Wu M, Hua R, Zhao M, Liu J, Xu G. 2003. Analysis of cigarette smoke condensates by comprehensive two-dimensional gas chromatography/time-of-flight mass spectrometry I acidic fraction. Anal Chem 75:4441-4451.

Mai Y, Higashi T, Terada K, Hatate C, Nepal P, Horiguchi M, Harada T, Miwa S, Horinouchi T. 2012. Nicotine- and tar-free cigarette smoke extract induces cell injury via intracellular Ca2+-dependent subtype-specific protein kinase C activation. J Pharmacol Sci 120:310-314.

Matsufuji Y, Yamamoto K, Yamauchi K, Mitsunaga T, Hayakawa T, Nakagawa T. 2013. Novel physiological roles for glutathione in sequestering acetaldehyde to confer acetaldehyde tolerance in Saccharomyces cerevisiae. Appl Microbiol Biotechnol 97:297-303.

Matsuo K, Ito H, Wakai K, Nagata C, Mizoue T, Tanaka K, Tsuji I, Tamakoshi A, Sasazuki S, Inoue M, Tsugane S. 2011. Cigarette smoking and pancreas cancer risk: an evaluation based on a systematic review of epidemiologic evidence in the Japanese population. Jpn J Clin Oncol 41:1292-1302.

Mazars C, Thuleau P, Lamotte O, Bourque S. 2010. Cross-talk between ROS and calcium in regulation of nuclear activities. Mol Plant 3:706-718.

McGough AM, Staiger CJ, Min JK, Simonetti KD. 2003. The gelsolin family of actin regulatory proteins: modular structures, versatile functions. FEBS Lett 552:75-81.

Mehta D, Ahmmed GU, Paria BC, Holinstat M, Voyno-Yasenetskaya T, Tiruppathi C, Minshall RD, Malik AB. 2003. RhoA interaction with inositol 1,4,5-trisphosphate receptor and transient receptor potential channel-1 regulates Ca2+ entry. Role in signaling increased endothelial permeability. J Biol Chem 278:33492-33500.

Messier EM, Bahmed K, Tuder RM, Chu HW, Bowler RP, Kosmider B. 2013. Trolox contributes to Nrf2-mediated protection of human and murine primary alveolar type II cells from injury by cigarette smoke. Cell Death Dis 4:e573.

Messier EM, Day BJ, Bahmed K, Kleeberger SR, Tuder RM, Bowler RP, Chu HW, Mason RJ, Kosmider B. 2013. N-acetylcysteine protects murine alveolar type II cells from cigarette smoke injury in a nuclear erythroid 2-related factor-2-independent manner. Am J Respir Cell Mol Biol 48:559-567.

Messner B, Frotschnig S, Steinacher-Nigisch A, Winter B, Eichmair E, Gebetsberger J, Schwaiger S, Ploner C, Laufer G, Bernhard D. 2012. Apoptosis and necrosis: two different outcomes of cigarette smoke condensate-induced endothelial cell death. Cell Death Dis 3:e424.

Nagamma T, Anjaneyulu K, Baxi J, Dayaram P, Singh P. 2011. Effects of cigarette smoking on lipid peroxidation and antioxidant status in cancer patients from Western Nepal. Asian Pac J Cancer Prev 12:313-316.

Numaga T, Nishida M, Kiyonaka S, Kato K, Katano M, Mori E, Kurosaki T, Inoue R, Hikida M, Putney JW Jr, Mori Y. 2010. Ca2+ influx and protein scaffolding via TRPC3 sustain PKCbeta and ERK activation in B cells. J Cell Sci 123:927-938.

Nunes P, Demaurex N. 2014. Redox regulation of store-operated Ca(2+) entry. Antioxid Redox Signa l21:915-32.

Park JW, Kim HP, Lee S.J., Wang X., Wang Y., Ifedigbo E., Watkins S.C., Ohba M., Ryter S.W., Vyas Y.M., Choi A.M., 2008. Protein kinase C alpha and zeta differentially regulate death-inducing signaling complex formation in cigarette smoke extract-induced apoptosis. J Immunol 180:4668-4678.

Pedersen SF, Owsianik G, Nilius B. 2005. TRP channels: an overview. Cell Calcium 38:233-252.

Poteser M, Schleifer H, Lichtenegger M, Schernthaner M, Stockner T, Kappe CO, Glasnov TN, Romanin C, Groschner K. 2011. PKC-dependent coupling of calcium permeation through transient receptor potential canonical 3 (TRPC3) to calcineurin signaling in HL-1 myocytes. PNAS 108:10556-10561.

Pryor WA, Stone K. 1993. Oxidants in cigarette smoke. Radicals, hydrogen peroxide, peroxynitrate, and peroxynitrite. Ann N Y Acad Sci 686:12-27.

Quintanar-Escorza MA, González-Martínez MT, del Pilar IO, Calderón-Salinas JV. 2010. Oxidative damage increases intracellular free calcium [Ca2+]i concentration in human erythrocytes incubated with lead. Toxicol In Vitro 24:1338-1346.

Rainey RP, Gillman IG, Shi X, Cheng T, Stinson A, Gietl D, Albino AP. 2009. Fluorescent detection of lipid peroxidation derived protein adducts upon in-vitro cigarette smoke exposure. Toxicol Mech Methods 19:401-409.

Rasmussen JE, Sheridan JT, Polk W, Davies CM, Tarran R. 2014. Cigarette smoke-induced Ca2+ release leads to cystic fibrosis transmembrane conductance regulator (CFTR) dysfunction. J Biol Chem 289:7671-7681.

Redondo PC, Harper MT, Rosado JA, Sage SO. 2006. A role for cofilin in the activation of store-operated calcium entry by de novo conformational coupling in human platelets. Blood 107:973-979.

Rivas FV, O'Keefe JP, Alegre ML, Gajewski TF. 2004. Actin cytoskeleton regulates calcium dynamics and NFAT nuclear duration. Mol Cell Biol 24:1628-1639.

Rizzuto R, De Stefani D, Raffaello A, Mammucari C. 2012. Mitochondria as sensors and regulators of calcium signalling. Nat Rev Mol Cell Biol 13:566-578.

Sabourin J, Harisseh R, Harnois T, Magaud C, Bourmeyster N, Déliot N, Constantin B. 2012. Dystrophin/α1-syntrophin scaffold regulated PLC/PKC-dependent store-operated calcium entry in myotubes. Cell Calcium 52:445-456.

Saleh SN, Albert AP, Large WA. 2009. Obligatory role for phosphatidylinositol 4,5-bisphosphate in activation of native TRPC1 store-operated channels in vascular myocytes. J Physiol 587:531-540.

Schweitzer KS, Hatoum H, Brown MB, Gupta M, Justice MJ, Beteck B, Van Demark M, Gu Y, Presson RG Jr, Hubbard WC, Petrache I. 2011. Mechanisms of lung endothelial barrier disruption induced by cigarette smoke: role of oxidative stress and ceramides. Am J Physiol Lung Cell Mol Physiol 301:L836-L846.

Shih RH, Cheng SE, Hsiao LD, Kou YR, Yang CM. 2011. Cigarette smoke extract upregulates heme oxygenase-1 via PKC/NADPH oxidase/ROS/PDGFR/PI3K/Akt pathway in mouse brain endothelial cells. J Neuroinflammation 8:104.

Su Y, Han W, Giraldo C, De Li Y, Block ER. 1998. Effect of cigarette smoke extract on nitric oxide synthase in pulmonary artery endothelial cells. Am J Respir Cell Mol Bio l19:819-825.

Suzuki YJ, Carini M, Butterfield DA. 2010. Protein carbonylation. Antioxid Redox Signal 12:323-325.

Tiruppathi C, Ahmmed GU, Vogel SM, Malik AB. 2006. Ca2+ signaling, TRP channels, and endothelial permeability. Microcirculation 13:693-708.

Tsuda S, Matsusaka N, Ueno S, Susa N, Sasaki YF. 2000. The influence of antioxidants on cigarette smoke-induced DNA single-strand breaks in mouse organs: a preliminary study with the alkaline single cell gel electrophoresis assay. Toxicol Sci 54:104-109.

U.S. Department of Health and Human Services. 2010. How Tobacco Smoke Causes Disease: The Biology and Behavioral Basis for Smoking-Attributable Disease: A Report of the Surgeon General. Atlanta, GA: U.S. Department of Health and Human Services, Centers for Disease Control and Prevention, National Center for Chronic Disease Prevention and Health Promotion, Office on Smoking and Health.

Valavanidis A, Vlachogianni T, Fiotakis K. 2009. Tobacco smoke: involvement of reactive oxygen species and stable free radicals in mechanisms of oxidative damage, carcinogenesis and synergistic effects with other respirable particles. Int J Environ Res Public Health 6:445-462.

van der Toorn M, Rezayat D, Kauffman HF, Bakker SJ, Gans RO, Koëter GH, Choi AM, van Oosterhout AJ, Slebos DJ. 2009. Lipid-soluble components in cigarette smoke induce mitochondrial production of reactive oxygen species in lung epithelial cells. Am J Physiol Lung Cell Mol Physiol 297:L109-L114.

van der Toorn M, Slebos DJ, de Bruin HG, Gras R, Rezayat D, Jorge L, Sandra K, van Oosterhout AJ. 2013. Critical role of aldehydes in cigarette smoke-induced acute airway inflammation. Respir Res 14:45.

Vanoverberghe K, Lehen'kyi V, Thébault S, Raphaël M, Vanden Abeele F, Slomianny C, Mariot P, Prevarskaya N. 2012. Cytoskeleton reorganization as an alternative mechanism of store-operated calcium entry control in neuroendocrine-differentiated cells. PLoS One 7:e45615.

Wang L, Zhao Y, Gui B, Fu R, Ma F, Yu J, Qu P, Dong L, Chen C. 2011. Acute stimulation of glucagon secretion by linoleic acid results from GPR40 activation and [Ca2+]i increase in pancreatic islet {alpha}-cells. J Endocrinol 210:173-179.

Wu M, Wu X, De Camilli P. 2013. Calcium oscillations-coupled conversion of actin ravelling waves to standing oscillations. PNAS 110:1339-1344.

Wu YN, Yang YC, Wagner PD. 1992. Modification of chromaffin cells with pertussis toxin or N-ethylmaleimide lowers cytoskeletal F-actin and enhances Ca(2+)-dependent secretion. J Biol Chem 267:8396-8403.

Xie XT, Liu Q, Wu J, Wakui M. 2009. Impact of cigarette smoking in type 2 diabetes development. Acta Pharmacol Sin 30:784-787.

Yang Z, Harrison CM, Chuang GC, Ballinger SW. 2007. The role of tobacco smoke induced mitochondrial damage in vascular dysfunction and atherosclerosis. Mutat Res 621:61-74.

Yao X, Garland CJ. 2005. Recent developments in vascular endothelial cell transient receptor potential channels. Circ Res 97:853-863.

Ye H, Ma WL, Jin S, Liu SY, Wang DX, Hu QH. 2008. Cigarette smoke extract activates PKC isoforms and down-regulates the expressions of potassium channels BK(Ca) and Kv1.5 in rat bronchial smooth muscle cells. Sheng Li Xue Bao 60:709-714.

Yoshida T, Tuder RM. 2007. Pathobiology of cigarette smoke-induced chronic obstructive pulmonary disease. Physiol Rev 87:1047-1082.

Yu LX, Dzikovski BG, Freed JH. 2012. A protocol for detecting and scavenging gas-phase free radicals in mainstream cigarette smoke. J Vis Exp 59:e3406.

Figure legends

Fig. 1. Dose-dependent effects of CSE on F-actin content and morphology changes in human endothelial EA.hy926 cells. After treatment without or with 1%, 5%, or 10% CSE for 4 h, cells were stained with rhodamine-phalloidin. (A) Representative fluorescent microscopic images of cells treated with different concentrations of CSE are shown. (B) Quantification of signals in fluorescence microscopy images of cells. (Cell shape changes were determined by fluorescence signals and were analyzed as described in the Methods.) The data are means ± SE of three independent experiments.

Fig. 2. Time-course effects of CSE on F-actin content and morphological changes in human endothelial EA.hy 926 cells. Cells were treated without or with 10% CSE for 1, 2, or 4 h and the relative F-actin contents (A) and cell shape changes (B) were measured as described in the legend to Fig. 1. The data are means ± SE of three independent experiments.

Fig. 3. Effects of thiol-containing compounds on CSE-induced cell shape changes in human endothelial EA.hy926 cells. Cells were treated with *N*-acetyl cysteine (NAC) (A), glutathione (GSH) (B), or lipoic acid (LA) (C) 30 min before exposed to 10% CSE for 4 h. After treatment, the cell shape changes were scored by fluorescence microscopy as described in the legend to Fig. 1.

Fig. 4. Protection by free-radical scavengers against CSE-induced cell shape changes. Endothelial EA.hy926 cells were treated with vitamin C (Vit C) (A), vitamin E (Vit E) (B), or aminoguanidine (AG) (C) 30 min before exposure to 10% CSE for 4 h. Changes in the cell shape were scored by fluorescence microscopy as described in the legend to Fig. 1.

Fig. 5. Effect of calcium chelators and store-operated channel (SOC) calcium entry inhibitor on CSE-induced cell shape changes. EA.hy926 cells were treated with the cell-impermeable calcium chelator EGTA (A), the cell-permeable chelator BAPTA-AM AM (B), or the SOC inhibitor MRS 1845 (C) 30 min before exposure to 10% CSE for 4 h. After treatment, the cell shape changes were visualized and scored by fluorescence microscopy as described in the legend to Fig. 1.

Fig. 6. Effect of CSE on intracellular calcium ion concentration in human endothelial EA.hy926 cells. Cells were treated without or with 2.5%, 5%, or 10% CSE for 8 h and the intracellular free Ca^{2+} was measured by loading the cells with 4 μM of Fluo-3 AM. The fluorescence intensity was measured by use of a fluorescence microscope (Zeiss, Axioskop 2). Values are the mean ± SEM, n=3.

Fig. 7. Effect of calcium chelators and store-operated channel (SOC) calcium entry inhibitor on CSE-induced intracellular calcium ion increase in human endothelial EA.hy926 cells. Cells were treated with the cell-permeable chelator BAPTA-AM AM (5 or 10 μM) (A), the cell-impermeable calcium chelator EGTA (1 or 2 mM) (B), or the SOC inhibitor MRS 1845 (C) 30 min before exposure to 5% CSE for 8 h. The intracellular free Ca^{2+} concentration was measured as described in the legend to Fig. 6. Values are the mean ± SEM, n=3.

Fig. 8. Effect of protein kinase C, phospholipase C, and inositol-1,4,5-trisphosphate receptor inhibitors on the

CSE-induced increase in the intracellular calcium concentration. EA.hy926 cells were treated with the protein kinase C inhibitor GF109203 (GF) (0.5 or 1 μM) (A), the phospholipase C inhibitor U-73122 (5 or 10 μM) (B), or the inositol-1,4,5-trisphosphate (IP3) receptor inhibitor xestospongin C (XeC) (5 or 10 microM) (C) 30 min before exposure to 5% CSE for 8 h. Intracellular free Ca^{2+} was measured as described in the legend to Fig. 6. Values are the mean ± SEM, n=3.

Fig. 9. Hypothetical signaling pathway of CSE-induced elevation of cytosolic Ca^{2+} ions and cell shrinkage. CSE exposure may trigger oxidative stress in cell membrane and then activate phospholipase C (PLC) enzyme. Activated PLC not only cleaves phosphatidylinositol 4,5-bisphosphate (PIP2) in order to produce inositol 1,4,5-trisphosphate (IP3) and diacylglycerol (DAG), but also induces the dissociation of transient receptor potential canonical type (TRPC) channels from PIP2. IP3 subsequently binds to IP3 receptor (IP3R) channels on membranes of the endoplasmic reticulum (ER) and stimulates the release of calcium ions (Ca^{2+}) into the cytosol. This calcium, either alone or combined with DAG, can activate the conventional and novel isoforms of PKC. Thereafter, the activated protein kinase C (PKC) phosphorylates TRPC and causes a massive and rapid influx of calcium into the cell. Both Ca^{2+} release from intracellular stores and Ca^{2+} influx through TRPC channels increase cytosolic Ca^{2+} levels significantly in human endothelial cells under exposure to CSE. Ultimately, Ca^{2+} signals acts upon the actin cytoskeleton and the cell shrinkage. TRPC-PIP2: the complex of TRPC channel and PIP2, $[Ca^{2+}]$cyto; cytosolic Ca^{2+} concentration, $[Ca^{2+}]_{ER}$: endoplasmic reticulum Ca^{2+} concentration; $[Ca^{2+}]$extra: extracellular Ca^{2+} concentration.

Fig. 1

(A)

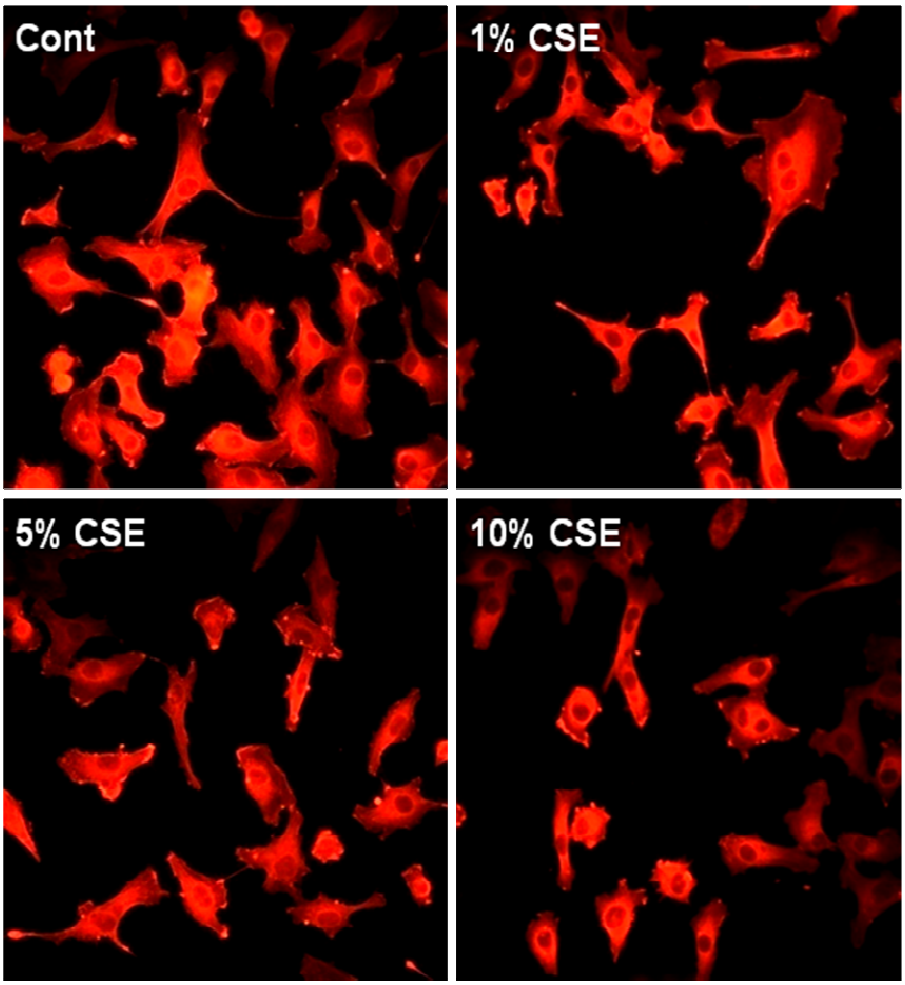

(B)

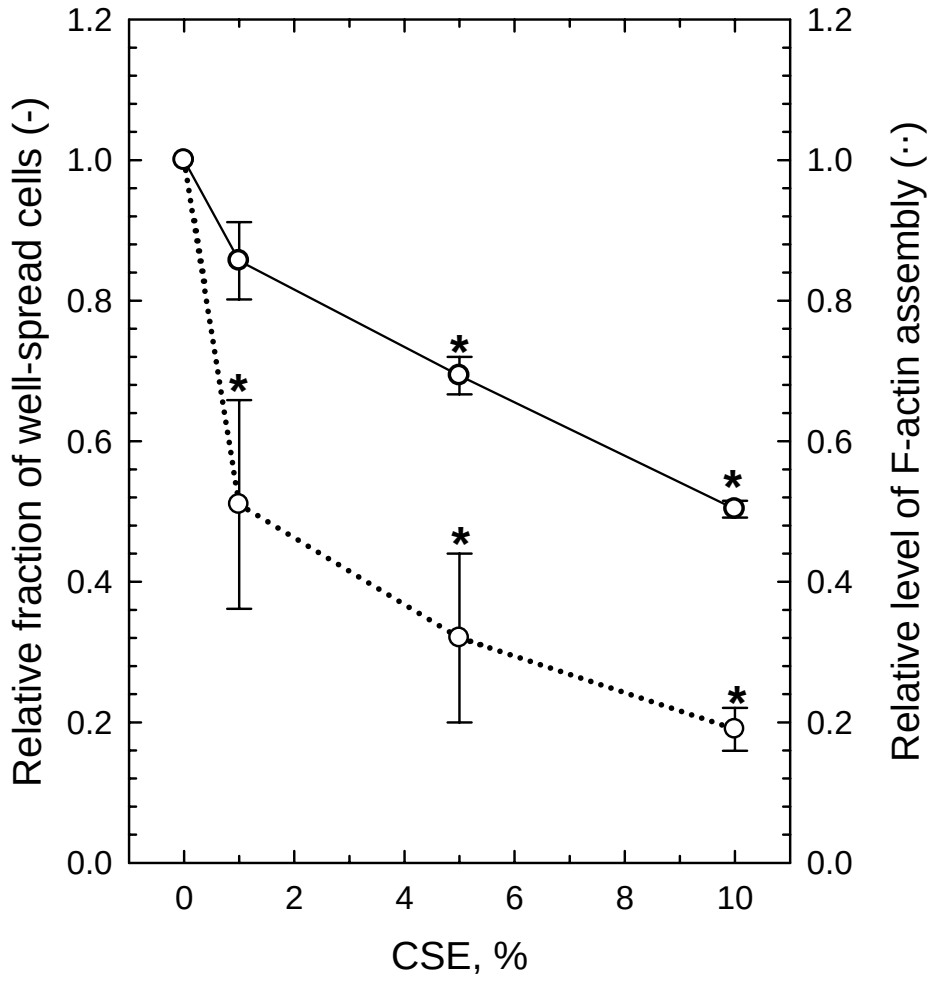
Relative fraction of well-spread cells (-)
Relative level of F-actin assembly (··)
CSE, %
0.0
0.2
0.4
0.6
0.8
1.0
1.2
0
2
4
6
8
10
*

Fig. 2

(A)

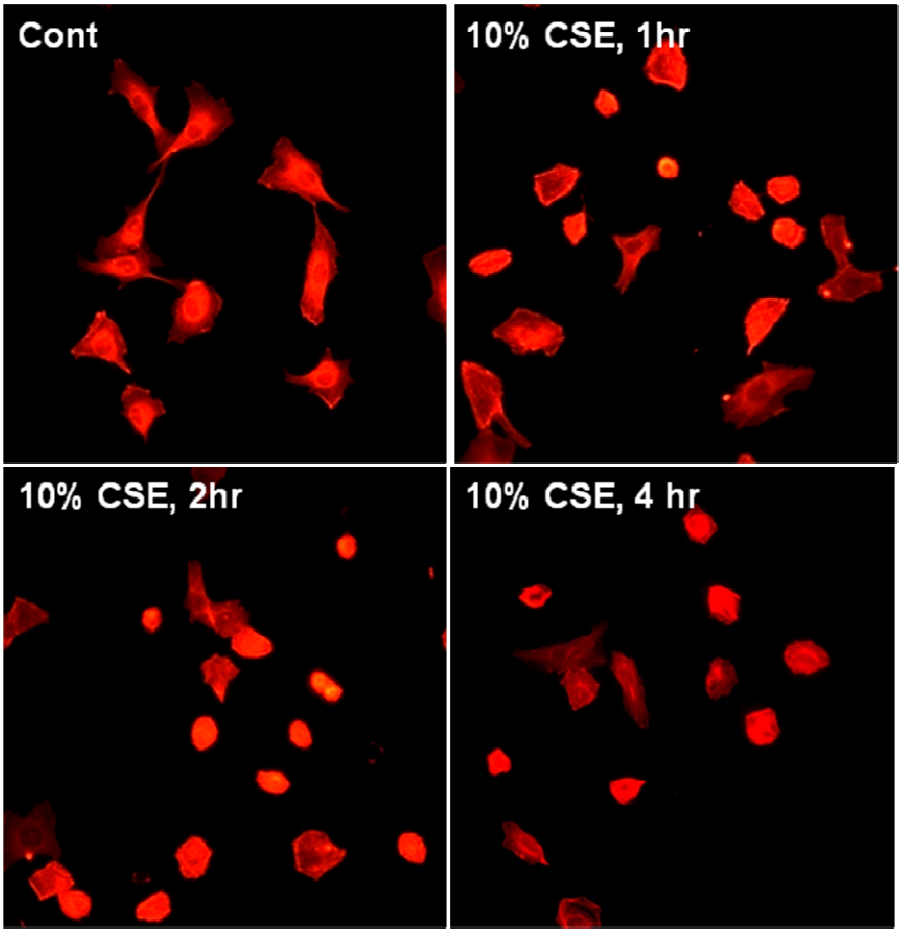

(B)

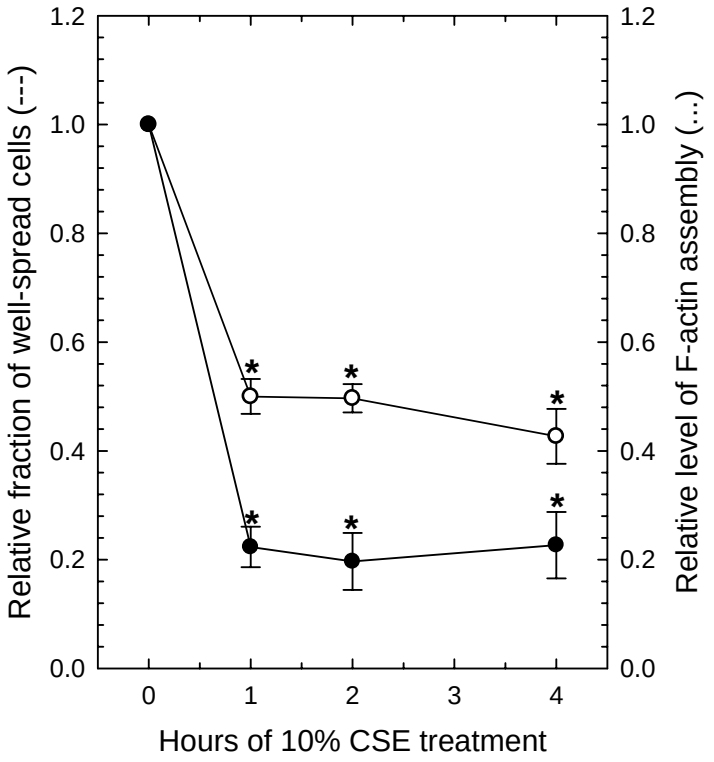
Relative fraction of well-spread cells (---)
Relative level of F-actin assembly (...)
Hours of 10% CSE treatment
0.0
0.2
0.4
0.6
0.8
1.0
1.2
0
1
2
3
4
*

Fig. 3

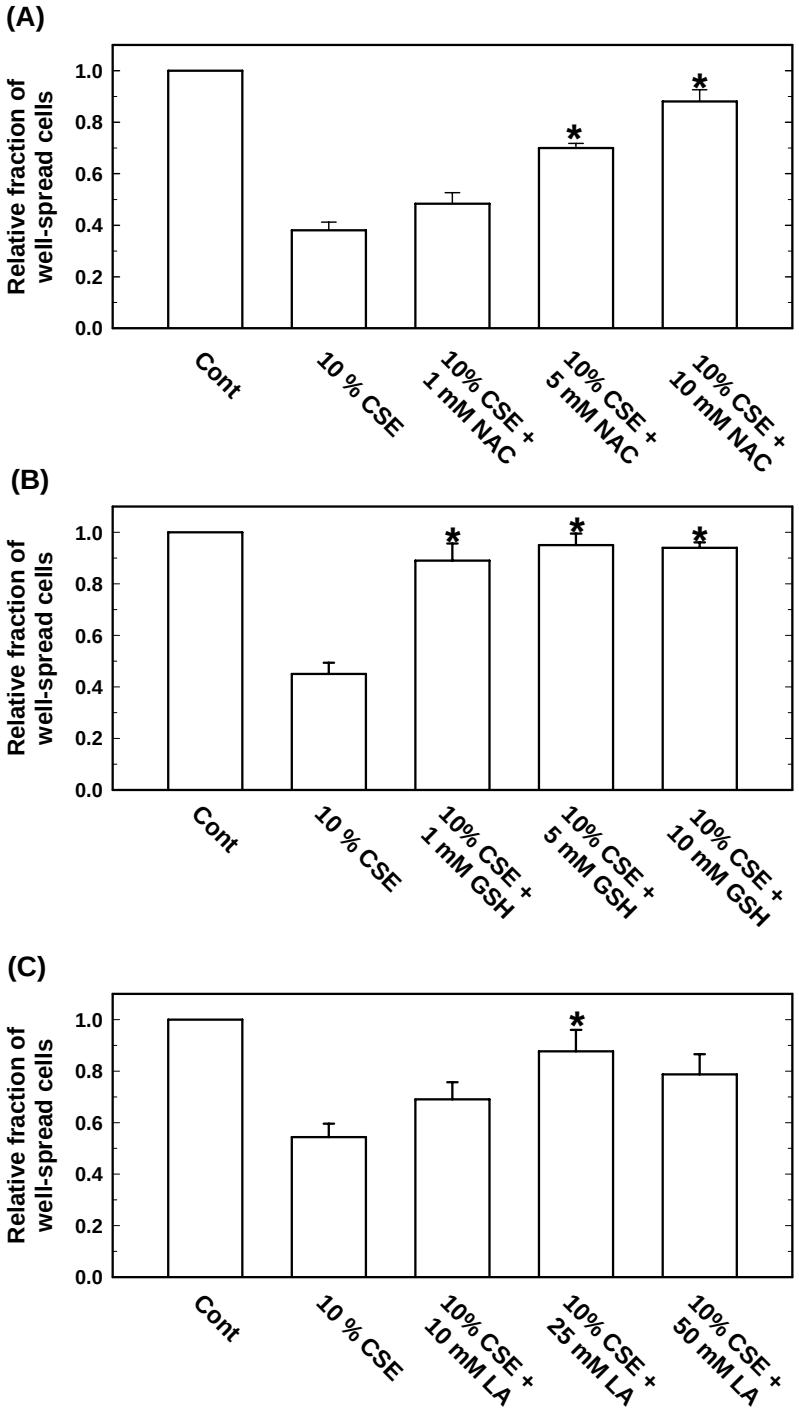
(A)
Relative fraction of well-spread cells
1.0
0.8
0.6
0.4
0.2
0.0
*
*
Cont
10 % CSE
10% CSE + 1 mM NAC
10% CSE + 5 mM NAC
10% CSE + 10 mM NAC
(B)
Relative fraction of well-spread cells
1.0
0.8
0.6
0.4
0.2
0.0
*
*
*
Cont
10 % CSE
10% CSE + 1 mM GSH
10% CSE + 5 mM GSH
10% CSE + 10 mM GSH
(C)
Relative fraction of well-spread cells
1.0
0.8
0.6
0.4
0.2
0.0
*
Cont
10 % CSE
10% CSE + 10 mM LA
10% CSE + 25 mM LA
10% CSE + 50 mM LA

Fig. 4

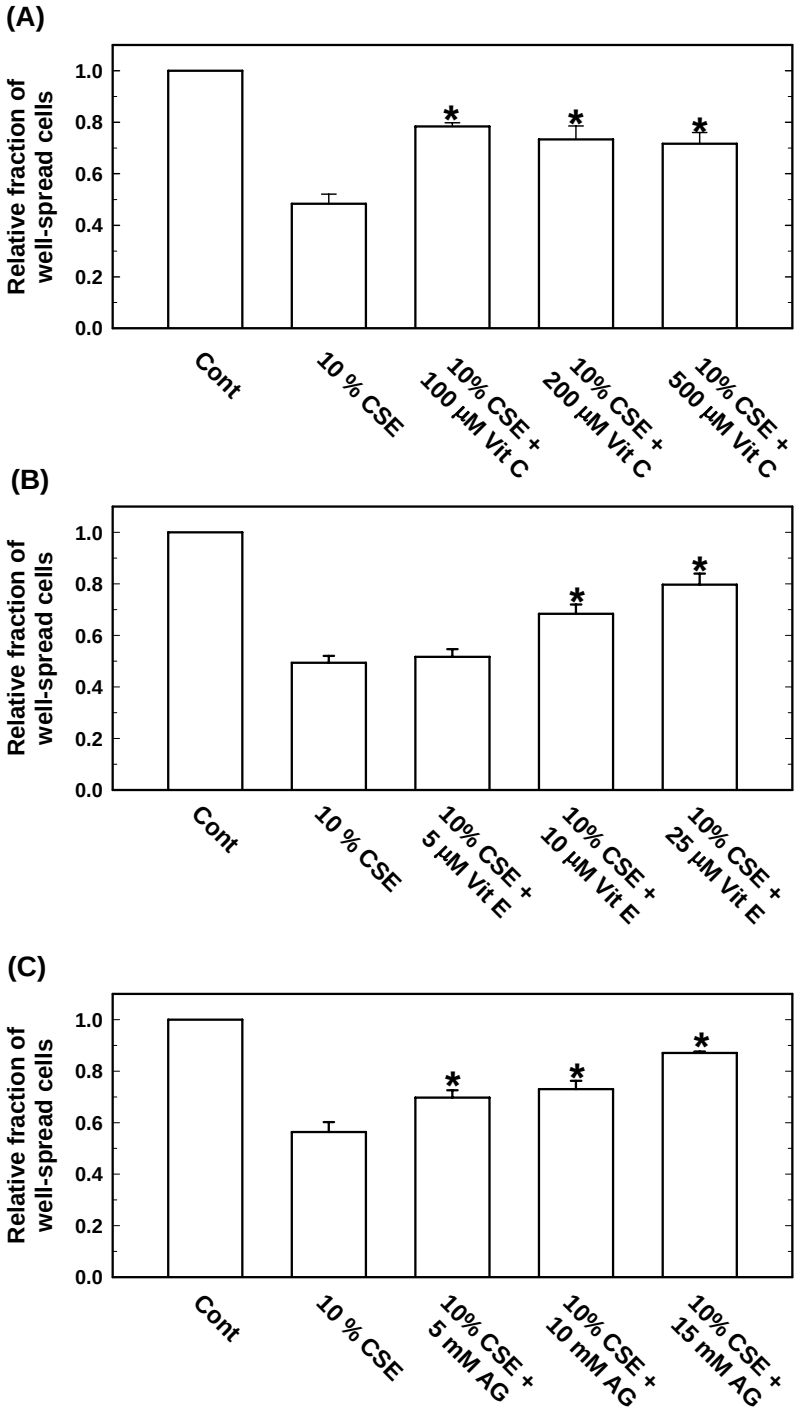
(A)
Relative fraction of well-spread cells
1.0
0.8
0.6
0.4
0.2
0.0
Cont
10 % CSE
10% CSE + 100 μM Vit C
10% CSE + 200 μM Vit C
10% CSE + 500 μM Vit C
(B)
Relative fraction of well-spread cells
1.0
0.8
0.6
0.4
0.2
0.0
Cont
10 % CSE
10% CSE + 5 μM Vit E
10% CSE + 10 μM Vit E
10% CSE + 25 μM Vit E
(C)
Relative fraction of well-spread cells
1.0
0.8
0.6
0.4
0.2
0.0
Cont
10 % CSE
10% CSE + 5 mM AG
10% CSE + 10 mM AG
10% CSE + 15 mM AG

Fig. 5

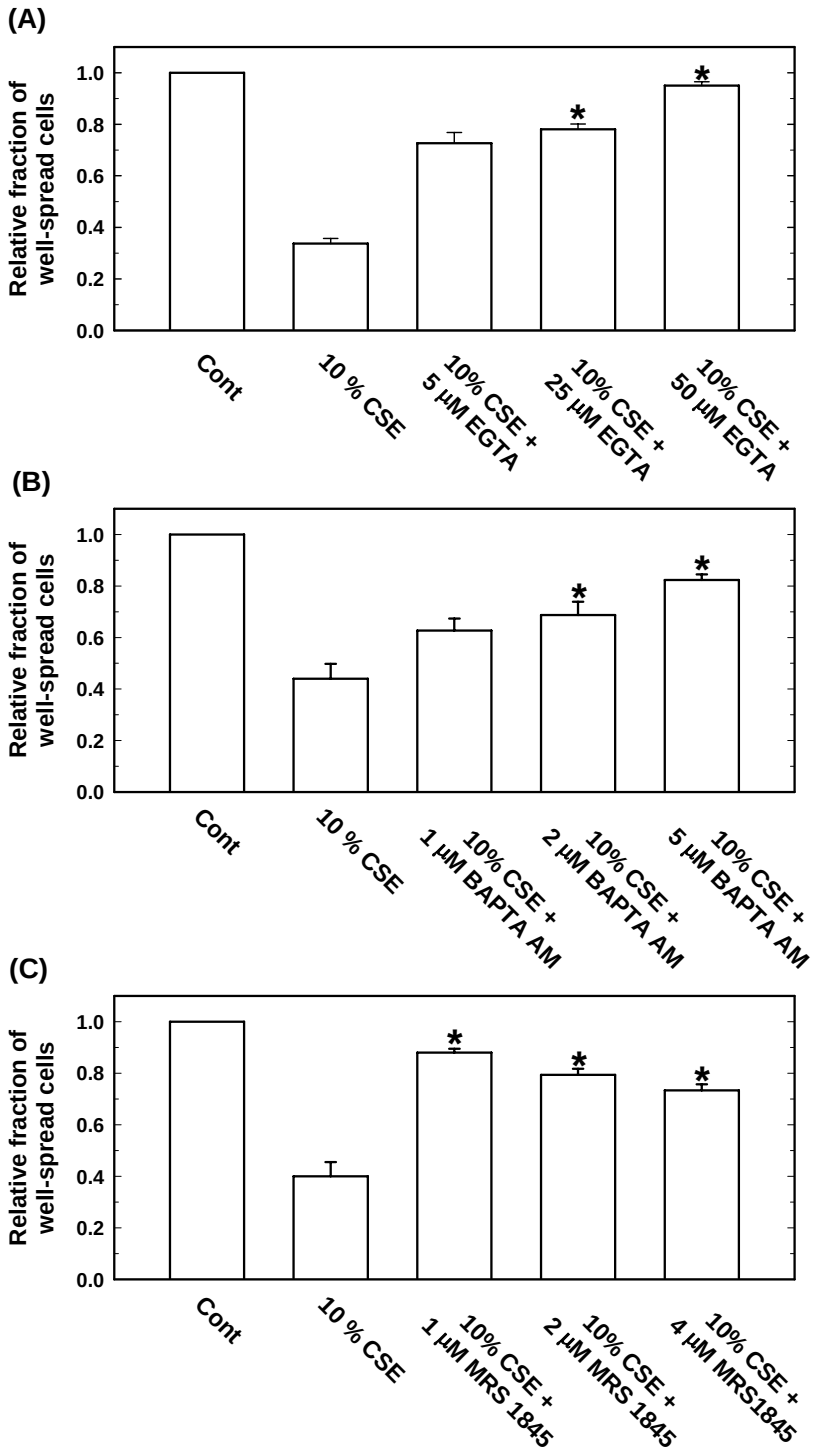
(A)
Relative fraction of well-spread cells
1.0
0.8
0.6
0.4
0.2
0.0
*
*
*
Cont
10 % CSE
10% CSE + 5 μM EGTA
10% CSE + 25 μM EGTA
10% CSE + 50 μM EGTA
(B)
Relative fraction of well-spread cells
1.0
0.8
0.6
0.4
0.2
0.0
*
*
Cont
10 % CSE
10% CSE + 1 μM BAPTA AM
10% CSE + 2 μM BAPTA AM
10% CSE + 5 μM BAPTA AM
(C)
Relative fraction of well-spread cells
1.0
0.8
0.6
0.4
0.2
0.0
*
*
*
Cont
10 % CSE
10% CSE + 1 μM MRS 1845
10% CSE + 2 μM MRS 1845
10% CSE + 4 μM MRS1845

Fig. 6

(A)

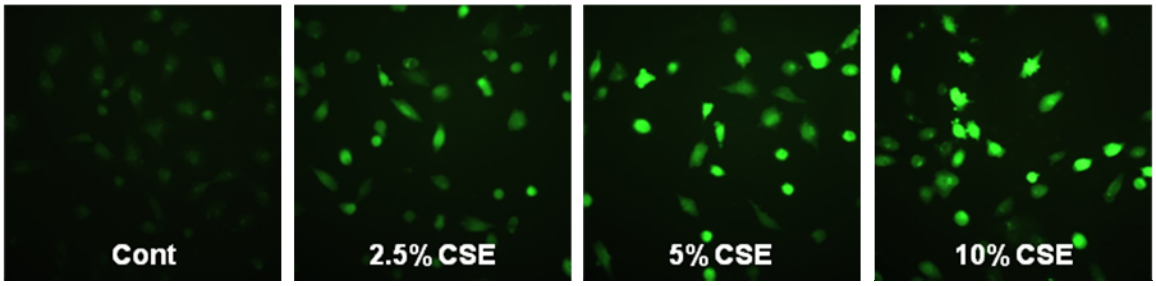
Cont
2.5% CSE
5% CSE
10% CSE

(B)

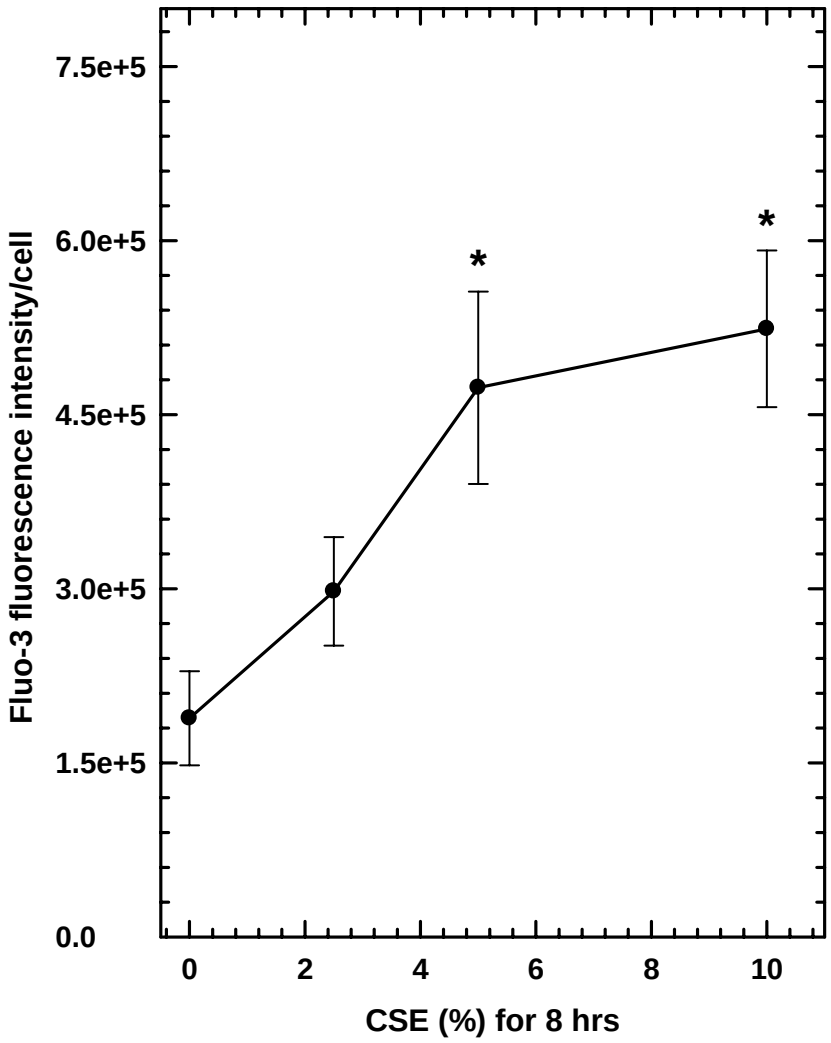
Fluo-3 fluorescence intensity/cell
7.5e+5
6.0e+5
4.5e+5
3.0e+5
1.5e+5
0.0
0
2
4
6
8
10
CSE (%) for 8 hrs
*
*

Fig. 7

(A)

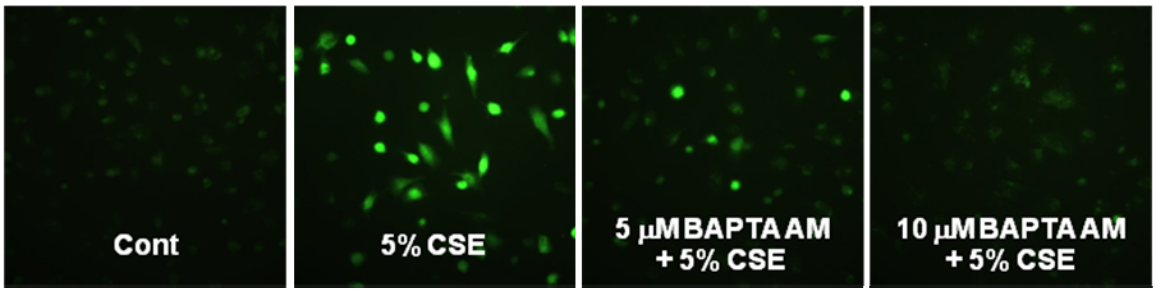
Cont
5% CSE
5 μM BAPTA AM
+ 5% CSE
10 μM BAPTA AM
+ 5% CSE

(B)

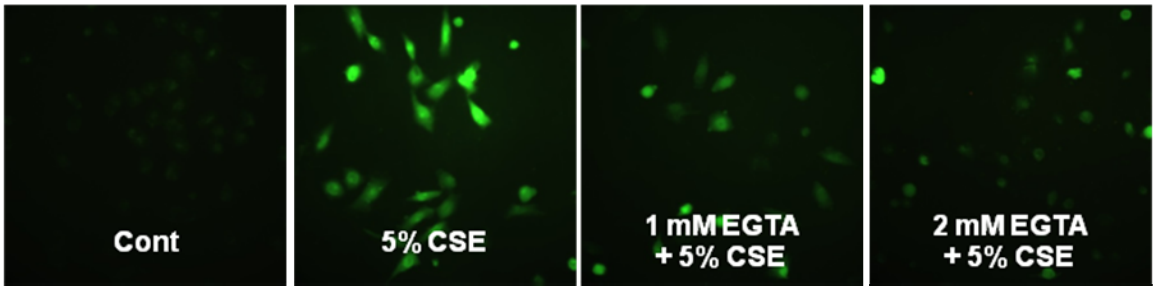
Cont
5% CSE
1 mM EGTA
+ 5% CSE
2 mM EGTA
+ 5% CSE

(C)

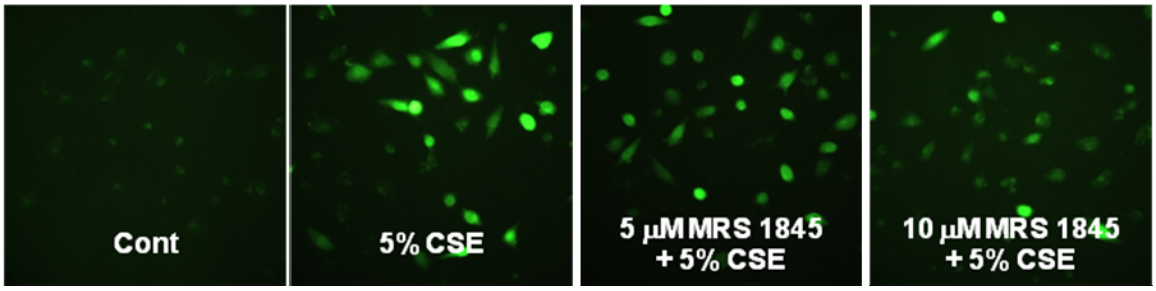
Cont
5% CSE
5 μM MRS 1845
+ 5% CSE
10 μM MRS 1845
+ 5% CSE

Fig. 8

(A)

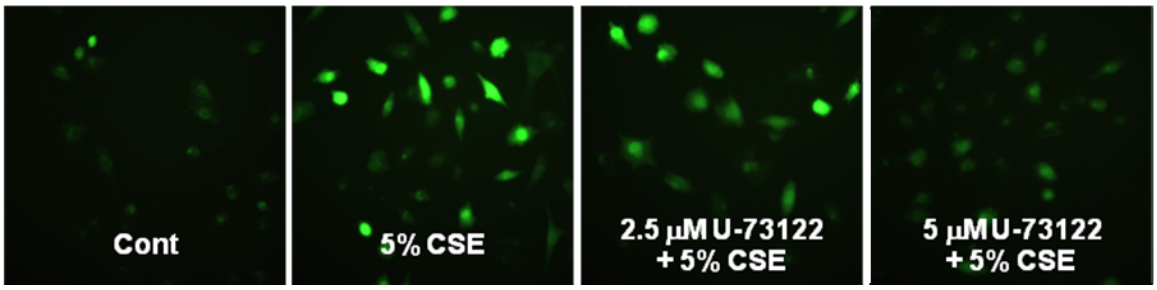
Cont
5% CSE
2.5 μM U-73122
+ 5% CSE
5 μM U-73122
+ 5% CSE

(B)

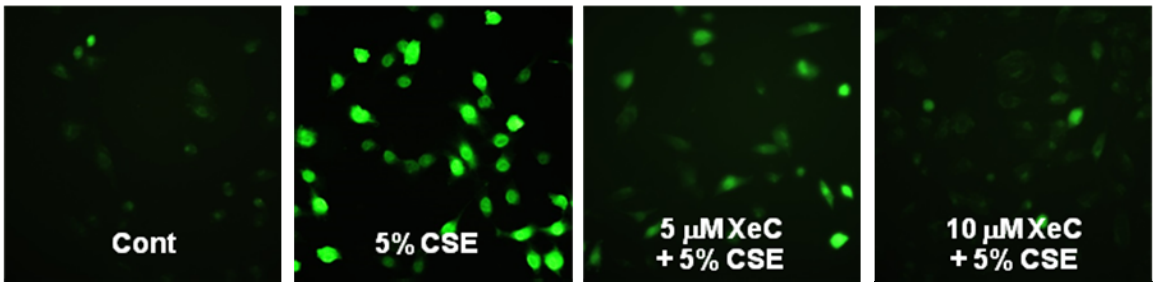
Cont
5% CSE
5 μM XeC
+ 5% CSE
10 μM XeC
+ 5% CSE

(C)

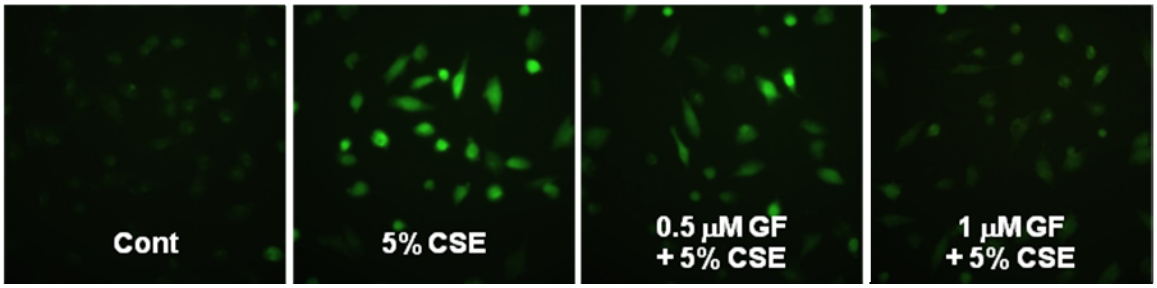
Cont
5% CSE
0.5 μM GF
+ 5% CSE
1 μM GF
+ 5% CSE

Fig. 9

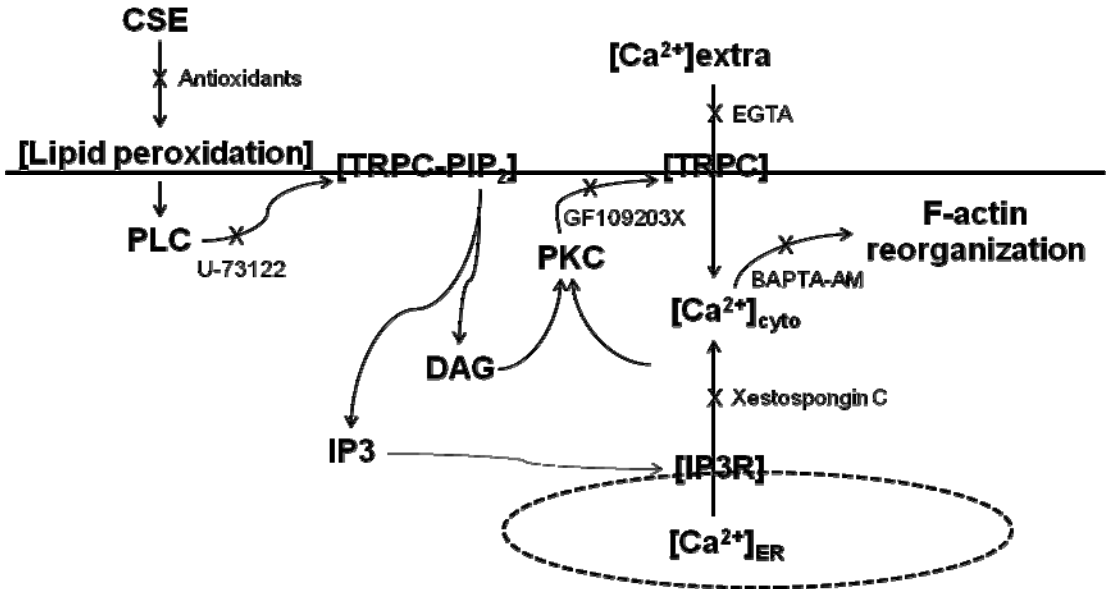
CSE
Antioxidants
[Lipid peroxidation]
[TRPC-PIP2]
[Ca2+]extra
EGTA
[TRPC]
PLC
U-73122
GF109203X
PKC
F-actin
reorganization
BAPTA-AM
[Ca2+]cyto
DAG
Xestospongin C
IP3
[IP3R]
[Ca2+]ER

科技部補助專題研究計畫出席國際學術會議心得報告

日期：103 年 10 月 31 日

計畫編號	MOST 101－2320－B－040－019－MY2		
計畫名稱	香菸煙霧水提取物造成人類血管內皮細胞及斑馬魚幼蟲發炎特性及保健防治研究		
出國人員姓名	王祖興	服務機構及職稱	中山醫學大學/教授
會議時間	102 年 08 月 18 日 至 102 年 08 月 21 日	會議地點	日本/千葉
會議名稱	(中文)日本第十屆亞太區煙草或健康大會 (英文) The 10th Asia Pacific Conference on Tobacco or Health		
發表題目	(中文)香菸煙霧提取物在人類內皮細胞造成微絲骨架重組之機制 (英文) Mechanism of cigarette smoke extract-induced reorganization of the actin cytoskeleton in human EA.hy926 endothelial cells		

一、參加會議經過

會議前一日由台中出發桃園國際機場，搭機前往日本成田機場，抵達後轉巴士前往千葉縣旅館，隔日至大會會場(幕張國際展覽中心)完成註冊並領取大會手冊(議程及摘要)及識別牌，之後展開三日的研習活動，課餘時間並走訪幕張臨近的海灘。本次會議約有 1000 人參與，分別來自 40 餘國，有 100 場的口頭演講及 380 餘幅的壁報論文，研討主題包括防止接觸菸草烟霧、抽菸與口腔健康、抽菸與心臟疾病、抽菸與肺结核、抽菸與呼吸道疾病等 19 種，我的主持任務及口頭演講安排在”抽菸與心臟疾病”主題，時間在會議的第二天。

二、與會心得

1. 會議的舉行安排包括會場佈、飲食及專業議程，均有相當高的水準，放置在會場的巨型人類肺臟仿真模型，讓整個會議的充滿了為人類呼吸系統健康打拼的使命感。
2. 本次參與會議非常難得與 Hisayoshi Fujiwara 教授共同主持第四分組的研討，並在會中發表本人最近有相關香菸煙霧提取物曝露對人類血管細胞造成危害之重要發現，在討論中除得到許多對個人研究的寶貴意見外，也與國際研究者建立難得的有誼，深感收穫滿滿，不虛此行，當然也感謝科技部對本次參與國際會議的相關經費補助。

三、發表論文摘要

Cigarette smoking is a major cause of cardiovascular disorders. Actin cytoskeleton is a possible key player in responding to inflammatory stimuli and also an early target of cellular oxidative stress. Laboratory previous results also show that cigarette smoke extract (CSE) induces rapid actin cytoskeleton remodeling and up-regulate ICAM-1 (intercellular adhesion molecule-1) expression in human umbilical vein endothelial cells (HUVEC). The purpose of this study is to understand the actin damages and its possible mechanism in human umbilical vein endothelial cells EA.hy926 exposed to cigarette smoke extract (CSE). The results showed that CSE caused dose- and time-dependent reorganization of actin cytoskeleton and cell shrinkage in EA.hy926 cells by staining with rhodamine phalloidin. In addition, CSE increased total protein carbonylation in a dose-dependent manner. Cells co-treated with different chemical compounds, such as reactive oxygen species scavenger (vitamin C, alpha-tocopherol, lipoic acid, glutathione, N-acetylcysteine), reactive carbonyl scavengers (aminoguanidine), calcium chelator (ethylene glycol tetraacetic acid, BAPTA-AM), transient receptor potential cation channels inhibitor (MRS 1845), and autopgay inhibitor (3-methyladenine) with CSE caused different inhibition of actin reorganization, protein carbonylation, and cell shrinkage in CSE-treated EA.hy926 cells. Among these compounds, lipoic acid, glutathione, EGTA, and MRS 1845 were found to potently inhibit the CSE-induced actin cytoskeleton reorganization and cell shrinkage. Furthermore, immunofluorescence staining analysis showed that the autophagy marker LC3 protein (microtubule-associated protein 1 light chain 3) accumulated at cell cortex in CSE-treated cells. Collectively, these findings suggest that CSE-mediated ROS generation and Ca^{2+} influx increase through TRPC channels are the key factors that may cause reorganization of actin cytoskeleton and the subsequent cell shrinkage. In addition, CSE-induced inappropriate organization of the actin cytoskeleton may dysregulate autophagy by abnormal accumulation of LC3 proteins at cell cortex.

四、建議

舉辦研討會的成效多元，宗旨及長遠目標是極為重要地，而不是為舉辦而舉辦，無菸家園是各國控菸、反菸團體及政府共同的理想，雖然本次研討會仍是以學術為主的會議，但會中仍展出呈現精緻地日本文化及當地小學生的反菸繪圖，充分宣示該國對無菸家園地重視，並從小學生的紮根教育做起，作法值得借鏡。

五、攜回資料名稱及內容

第 10 屆大會手冊一種，內容包含詳細議程及發表論文摘要。

六、其他

科技部補助計畫衍生研發成果推廣資料表

日期:2014/10/31

科技部補助計畫	計畫名稱: 香菸煙霧水提取物造成人類血管內皮細胞及斑馬魚幼蟲發炎特性及保健防治研究
	計畫主持人: 王祖興
	計畫編號: 101-2320-B-040-019-MY2　　學門領域: 保健營養

無研發成果推廣資料

101 年度專題研究計畫研究成果彙整表

計畫主持人：王祖興	計畫編號：101-2320-B-040-019-MY2
計畫名稱：香菸煙霧水提取物造成人類血管內皮細胞及斑馬魚幼蟲發炎特性及保健防治研究	

成果項目			量化			單位	備註（質化說明：如數個計畫共同成果、成果列為該期刊之封面故事...等）
			實際已達成數（被接受或已發表）	預期總達成數(含實際已達成數)	本計畫實際貢獻百分比		
國內	論文著作	期刊論文	0	0	0%	篇	
		研究報告/技術報告	0	0	0%		
		研討會論文	0	0	0%		
		專書	0	0	0%		
	專利	申請中件數	0	0	0%	件	
		已獲得件數	0	0	0%		
	技術移轉	件數	0	0	0%	件	
		權利金	0	0	0%	千元	
	參與計畫人力（本國籍）	碩士生	0	0	0%	人次	
		博士生	1	0	100%		訓練博士生撰寫科技期刊發表之能力
		博士後研究員	0	0	0%		
		專任助理	1	1	100%		
國外	論文著作	期刊論文	0	1	0%	篇	研究論文已完成投稿 Environmental Toxicology,目前仍在審查中
		研究報告/技術報告	0	0	0%		
		研討會論文	1	1	100%		部份研究成果已在 2013 日本第十屆亞太區煙草或健康大會中以口頭演講方式發表
		專書	0	0	0%	章/本	
	專利	申請中件數	0	0	0%	件	
		已獲得件數	0	0	0%		
	技術移轉	件數	0	0	0%	件	
		權利金	0	0	0%	千元	
	參與計畫人力（外國籍）	碩士生	0	0	0%	人次	
		博士生	0	0	0%		
		博士後研究員	0	0	0%		
		專任助理	0	0	0%		

其他成果 (無法以量化表達之成果如辦理學術活動、獲得獎項、重要國際合作、研究成果國際影響力及其他協助產業技術發展之具體效益事項等，請以文字敘述填列。)	無

	成果項目	量化	名稱或內容性質簡述
科教處計畫加填項目	測驗工具(含質性與量性)	0	
	課程/模組	0	
	電腦及網路系統或工具	0	
	教材	0	
	舉辦之活動/競賽	0	
	研討會/工作坊	0	
	電子報、網站	0	
	計畫成果推廣之參與（閱聽）人數	0	

科技部補助專題研究計畫成果報告自評表

請就研究內容與原計畫相符程度、達成預期目標情況、研究成果之學術或應用價值（簡要敘述成果所代表之意義、價值、影響或進一步發展之可能性）、是否適合在學術期刊發表或申請專利、主要發現或其他有關價值等，作一綜合評估。

1. 請就研究內容與原計畫相符程度、達成預期目標情況作一綜合評估

■達成目標

□未達成目標（請說明，以 100 字為限）

□實驗失敗

□因故實驗中斷

□其他原因

說明：

2. 研究成果在學術期刊發表或申請專利等情形：

論文：□已發表 ■未發表之文稿 □撰寫中 □無

專利：□已獲得 □申請中 ■無

技轉：□已技轉 □洽談中 ■無

其他：（以 100 字為限）

3. 請依學術成就、技術創新、社會影響等方面，評估研究成果之學術或應用價值（簡要敘述成果所代表之意義、價值、影響或進一步發展之可能性）（以 500 字為限）

本研究以人類血管內皮細胞為模式，了解香菸煙霧提取物如何造成發炎(包含氧化傷害)相關之反應，發現香菸煙霧在血管內皮細胞造成明顯的 ROS 形成，活化 IP3R/PLC/PKC 訊息傳遞路徑，導致細胞內鈣離子濃度上升、微絲骨架重組及細胞外形的皺縮，這個現象與抽菸所導致的心血管疾病，包括血管炎、動脈粥狀硬化及高血壓等關係密切。因此，抑制鈣離子通道特別是抑制 TRPC 通道，從而防治抽菸所引起的心血管疾病可能是一重要的新策略，值得進一步證實，另外，本分析模型也是抑制 TRPC 通道藥物開發極為簡便的測試平台。